Phagocytosis Induced by Thyrotropin in Cultured Thyroid Cells Is Associated with Myosin Light Chain Dephosphorylation and Stress Fiber Disruption

William J. Deery* and Julian P. Heath‡

*Department of Medicine, Division of Endocrinology and Metabolism; and ‡Departments of Pediatrics, Children's Nutrition Research Center, and Cell Biology, Baylor College of Medicine, Houston, Texas 77030

Abstract. The actin/myosin II cytoskeleton and its role in phagocytosis were examined in primary cultures of dog thyroid cells. Two (19 and 21 kD) phosphorylated light chains of myosin (P-MLC) were identified by two-dimensional gel electrophoresis of antimyosin immunoprecipitates, and were associated with the Triton X-100 insoluble, F-actin cytoskeletal fraction. Analyses of Triton-insoluble and soluble $^{32}PO_4$-prelabeled protein fractions indicated that TSH (via cAMP) or TPA treatment of intact cells decreases the MLC phosphorylation state. Phosphoamino acid and tryptic peptide analyses of ^{32}P-MLCs from basal cells showed phosphorylation primarily at threonine and serine residues; most of the [^{32}P] appeared associated with a peptide containing sites typically phosphorylated by MLC kinase. Even in the presence of the agents which induced dephosphorylation, the phosphatase inhibitor, calyculin A, caused a severalfold increase in MLC phosphorylation at several distinct serine and threonine sites which was also associated with actomyosin and cell contraction. Phosphorylation of cell homogenate proteins or the cytoskeletal fraction with [γ-^{32}P]ATP indicated that Ca^{2+}, EGTA, or trifluoperazine (TFP) has little effect on the phosphorylation of MLC. Both fluorescent phalloidin and antimyosin staining of cells showed distinct dorsal and ventral stress fiber complexes which were disrupted within 30 min by TSH and cAMP; TPA appeared to cause disruption of dorsal, and rearrangement of ventral complexes. Concomitant with MLC dephosphorylation and stress fiber disruption, TSH/cAMP, but not TPA, induced dorsal phagocytosis of latex beads. While stimulation of either A or C-kinase disrupts dorsal stress fibers and rearranges actomyosin, another event(s) mediated by A-kinase appears necessary for phagocytic activity.

NONMUSCLE cells, including thyroid, contain actomyosin complexes that can provide the mechanochemical framework for a variety of dynamic processes such as cell shape changes, surface receptor mobility, secretion, and phagocytosis (14, 18, 30, 37). Similarities exist between nonmuscle and smooth muscle actomyosin structural components, and their regulation (31). Typically, myosins contain a regulatory light chain phosphoprotein (myosin light chain, MLC)[1] ranging between 18 and 22 kD (3, 21, 31); both serine 19 and threonine 18 residues of MLC can be phosphorylated (11, 38), although the rate and extent of threonine phosphorylation has been observed to be less than that of serine (11, 23). In cardiac (22), slow skeletal muscle (48), myeloid leukemia (42), macrophage (53), platelet (28), and bovine brain (36) cells, phosphorylated MLC isoforms have been identified by electrophoretic resolution.

MLC phosphorylation plays a key role in regulating actin–myosin interactions and contraction in both smooth muscle and nonmuscle cells (3, 13, 54). Dephosphomyosin exists mostly in a dimeric form, whereas phosphomyosin forms bipolar filaments (35, 45, 49) with increased affinity for filamentous actin and increased myosin ATPase activity (2, 35, 40, 46, 47). Phosphorylation of the MLC serine 19 residue occurs via a specific Ca^{2+}/calmodulin-stimulated kinase (MLC kinase; MLCK) (1, 4, 38, 56), whereas a Ca^{2+}-independent kinase(s) phosphorylates at a threonine residue as shown in brain (36), for example. Protein kinase C phosphorylates MLC, but at serine 1 and 2, and also threonine 9, which in vitro, can suppress ATPase activity stimulated by serine 19 phosphorylation (25).

Presently, little evidence exists for regulation of the MLC phosphorylation state at the phosphatase level, although a type-1 phosphatase appears to be involved in fibroblasts (16). There is consensus that increases in cAMP can antagonize MLC phosphorylation and contraction (7, 9, 12, 33, 43). Phosphorylation of MLCK by A-kinase (9, 12, 33) or C-kinase (24) inhibits its Ca^{2+}/calmodulin-stimulated activ-

1. *Abbreviations used in this paper*: CHES, 2-(cyclohexylamino)ethanesulfonic acid; F-actin, filamentous actin; MLC, myosin light chain; MLCK, MLC kinase; P-MLC, phosphorylated MLC; 2-D, two dimensional; TPA, 12-*o*-tetradecanoyl-phorbol-13-acetate; TSH, thyroid-stimulating hormone (or thyrotropin).

ity in vitro; such phosphorylation of MLCK by the former appears to be responsible for cAMP inhibition of contraction in retinal cones (9), and MLC dephosphorylation and stress fiber disruption in fibroblasts (33). Often, agonists that stimulate secretion and changes in cell shape will elevate intracellular Ca^{2+} and concomitantly increase MLC phosphorylation and actomyosin formation, as observed in platelets (17). In contrast, the thyroid agonist, (thyroid-stimulating hormone, TSH), elevates cAMP levels which induces phagocytosis of colloid or latex beads by thyroid cells (50), and causes a more rounded cell morphology, and acute disruption of F-actin complexes in these cultures (37, 41, 52, 55). It is not clear whether the C-kinase stimulating phorbol ester, 12-*o*-tetradecanoyl-phorbol-13-acetate (TPA), can promote phagocytosis, although epithelial cell shape changes and rearrangement of F-actin have been observed (29, 41, 44). The mechanisms involved in these cAMP and phorbol ester-mediated processes are unknown.

Our previous studies have shown that both TSH via cAMP (26) and TPA (27), decrease the phosphorylation state of 19- and 21-kD proteins in cultured dog thyroid cells. While these proteins appeared to be MLCs, inhibitors of intracellular Ca^{2+} or calmodulin failed to decrease the phosphorylation state of these proteins, thus questioning the involvement of a classic Ca^{2+}/calmodulin stimulated kinase. In the present report, immunoprecipitation combined with two dimensional (2-D) PAGE analysis has identified these proteins as MLCs which in basal cells are primarily phosphorylated at threonine and serine sites, and are associated with the detergent-insoluble cytoskeleton. Phosphorylation is independent of Ca^{2+}/calmodulin, and unlike the Ca^{2+}/calmodulin MLCK (9, 12, 33), is not directly inhibited by cAMP and A-kinase in vitro. However, regulation of the agonist-induced MLC dephosphorylation at a protein phosphatase 1 and/or 2A level is indicated since the phosphatase inhibitor, calyculin A, increases MLC phosphorylation severalfold over basal levels even in the presence of agents which have induced dephosphorylation. Both kinase and phosphatase activity are associated with the detergent-insoluble cell fraction. The data show that while TSH/cAMP and TPA-induced MLC dephosphorylations are associated with stress fiber disruption, the A-kinase, but not C-kinase, pathway significantly induces phagocytosis of latex beads.

Materials and Methods

Tissue Preparations and Incubations for [^{32}P]Phosphate Labeling

Cultures of dog thyroid follicle cells were prepared as previously described (37). Primary cultures were grown at 37°C in Coon's modified Ham's F-12 medium supplemented with 0.5% bovine calf serum (supplied by the Tissue Culture Core Laboratory of the Diabetes and Endocrinology Research Center of Baylor College of Medicine, Houston, TX), insulin (10 μg/ml), cortisol (3.6 μg/ml), transferin (5 μg/ml), glycyl-L-histidyl-L-lysine (0.2 μg/ml), somatostatin (10 μg/ml), and 1 mU/ml TSH (NIDDK-bTSH, 10–30 U/mg, supplied by the Pituitary Hormone Distribution Program of the National Institutes of Diabetes, Digestive and Kidney Diseases, Bethesda, MD) in a water-saturated atmosphere of 5% CO_2. Medium containing TSH was designated 6H. Confluent cells were generally used within 3 wk of culture, and before use were grown in Coon's medium without TSH (5H) for 48 h. When fibroblasts from thyroid tissue were used, 1-wk cultures grown in 5H medium were allowed to become routinely acidic. This procedure selectively caused thyroid cell detachment and cultures subsequently became predominantly fibroblastic.

Cultured thyroid cells (500–700 μg protein/35-mm dish) were incubated in 5% CO_2/air with 0.15 mCi/ml [^{32}P]orthophosphoric acid (supplied by the Molecular Endocrinology Core Laboratory of the Diabetes and Endocrinology Research Center of Baylor College of Medicine, Houston, TX) in phosphate-free Tyrode's buffer (15 mM Hepes, 136 mM NaCl, 2 mM KCl, 10 mM Na_2CO_3, 1 mM $MgCl_2$, 1 mg/ml glucose, 0.1 mM nonessential and essential amino acids, pH 7.4–7.5) at 37°C for 120 min. This was previously found to maximally label the intracellular [γ-^{32}P]ATP pools (26). Labeled cells were washed with the above buffer and incubated at 37°C in Tyrode's buffer with or without various agents and for the times indicated in the figures and table.

Separation of the Cytoskeletal and Cytosol Fractions

At appropriate times, incubations were terminated by removal of the buffer and a brief wash at 2°C with cytoskeletal lysis buffer containing 40 mM sodium pyrophosphate, 20 mM potassium phosphate, 10 mM sodium molybdate, and 3 mM EGTA, pH 7.4. Cells were then extracted by incubation in the above solution made 1% Triton X-100 (Sigma Immunochemicals, St. Louis, MO) for 3 min at 2°C. The material remaining on the dish after removal of the buffer (17, 26, 27) was considered as the detergent-insoluble cytoskeletal fraction; protein in the buffer fraction was considered as the cytosol fraction. Approximately 60% of the total protein was extracted and 40% remained in the cytoskeletal-containing fraction.

Myosin Extraction and Immunoprecipitation

Myosin was extracted from [^{32}P]phosphate-labeled cytoskeletons by incubating the detergent-insoluble material in 0.25 ml of extraction buffer containing 100 mM sodium pyrophosphate, 50 mM NaF, 5 mM EGTA, 15 mM 2-mercaptoethanol, 1.5 mM PMSF, 10 mM $MgCl_2$/ATP, 0.5 M KCl, and 10% glycerol, pH 8.8, at 4°C for 30 min. The buffer was removed and diluted fourfold with 50 mM Tris, 190 mM NaCl, 6 mM EDTA, 0.1% trasylol, 1.25% Triton X-100, pH 7.4, containing aliquots of thymus myosin antibody (kindly supplied by Dr. John Kendrick-Jones, Cambridge, England), and incubated for 90 min at 2°C. After a brief microfuge clarification spin, 100 μl of protein A–Sepharose CL-4B (Pharmacia, Uppsala, Sweden): H_2O suspension (1:1) was added to the supernatant and incubated for 40 min at 25°C with shaking. The protein A–Sepharose was then pelleted and washed twice with 1 ml of dilution buffer and 1.5 mM PMSF at 25°C for 30 min each. A third wash was done in dilution buffer without Triton, and the pelleted protein A–Sepharose was incubated in isoelectric focusing sample buffer containing 9 M urea, 4% NP-40 (Sigma Immunochemicals), 2% 2-mercaptoethanol, 4% 3.5–10 ampholine (LKB Bromma, Sweden) for 2 h at 25°C. After protein solubilization, the sepharose was pelleted and the supernatant subjected to 2-D electrophoresis. For analysis of the crude extracted myosin fraction, the 0.25 ml sample was diluted with 1.8 ml of urea isoelectric focusing buffer, incubated at 25°C for 2 h and concentrated using Centricon-10 microconcentrators (Amicon Corp., Danvers, MA).

Gel Electrophoretic Analyses

When 1-D SDS-PAGE was used, protein was solubilized by boiling for 3 min in 2% SDS, 5% 2-mercaptoethanol, 10% glycerol, 0.002% bromphenol blue, and 62.5 mM Tris-HCl, pH 6.8. When homogenates were analyzed, 4× sample buffer was used. Samples (30–60 μg) were subjected to electrophoresis, with 3% acrylamide (Bio Rad Labs, Hercules, CA) in the stacking gel and a 5–18% acrylamide gradient in the resolving gel according to the method of Laemmli (32). Two dimensional PAGE was performed according to the methods of Anderson et al. (5) and Dunbar (15). Samples were solubilized in either 9 M urea, 4% NP-40, 2% 2-mercaptoethanol, 4% 3.5–10 ampholine, or 0.05 M 2-(cyclohexylamino)ethane-sulfonic acid (CHES) (Calbiochem Corp., San Diego, CA), 2% SDS, 10% glycerol, 2% 2-mercaptoethanol (5, 15), and after isoelectric focusing, resolved according to molecular weight on either 11% acrylamide or 5–20% acrylamide gradient gels. For homogenate studies, reactions were terminated and the protein solubilized by addition of 4× CHES-SDS sample buffer and boiled for 3 min. All gels were stained with Coomassie blue in methanol, H_2O, acetic acid (5:5:1), destained, dried, and subjected to autoradiography at −70°C using XAR-5 or XS-5 film (Eastman Kodak Co., Rochester, NY) and two Dupont lighting plus BE intensifying screens (Dupont/NEN, Wilmington, DE). The relative amounts of radioactivity in phosphoproteins were determined by integration of densitometric scans of autoradiograms using a Quick Scan, Jr. TLC plus (Helena Laboratories, Beaumont, TX).

2-D Tryptic Phosphopeptide Mapping and Phosphoamino Acid Analyses

Cultured thyroid cells in 35-mm dishes were loaded with 0.8 mCi/ml [^{32}P]phosphate in Tyrode's buffer without $CaCl_2$ for 2 h at 37°C, washed and incubated without or with 40 mU/ml TSH, 0.2 μM TPA, or 400 nM calyculin A (L C Services Corp., Woburn, MA) for 20 min. Cells were then lysed as described above, and cytoskeletal fractions were subjected to 2-D electrophoresis and the Coomassie-stained MLC spots excised from the gels. In vitro phosphorylation of ATP-extracted cytoskeletal myosin using purified C-kinase (Calbiochem Corp.) was done to provide a standard for identifing MLC tryptic phosphopeptides and phosphorylation sites. The Triton-insoluble cytoskeletal fraction was incubated for 4 min at 2°C in 220 μl of a buffer containing 30 mM Tris-HCl, pH 7.5, 1.2 mM $CaCl_2$, 5 mM $MgCl_2$, 1 mM EGTA, 45 mM KCl, 0.5 mM DTT, 0.5 mM ATP, 150 μg/ml phosphatidylserine (Sigma Immunochemicals, St. Louis, MO), 0.2 μM TPA. Buffer containing extracted myosin was removed, and to 50-μl aliquots was added 0.1 μg protein kinase C and [γ-^{32}P]ATP (2,000 cpm/pmol). Phosphorylation was carried out at 25°C for 1 h, and reactions were terminated by the addition of 4× SDS sample buffer. [^{32}P]MLC from excised gel pieces was digested first by washing the pieces in 50 then 80% methanol followed by 20 mM ammonium bicarbonate (8). Gels were incubated in 50 mM ammonium bicarbonate containing 20 μg TPCK trypsin (Worthington Biochemical Corp., Freehold, NJ) at 37°C for 2 h. Two fresh trypsin aliquots were added 2 h apart, followed by an overnight incubation. Peptide digest solutions were then lyophilized, and the phosphotryptic peptides resolved essentially as described (28). Electrophoresis was performed on cellulose thin-layer sheets 20 × 20 cm/0.1 mm thick (E. Merck Reagents, Darmstadt, W. Germany) in acetic acid/formic acid/H_2O (15:5:80) for 40 min at 700 V, followed by chromatographic resolution in the second dimension in *n*-butyl alcohol/pyridine/acetic acid/H_2O (156:120:24:96). Phosphopeptide spots were detected by autoradiography with Kodak XAR-5 film (Eastman Kodak Co.), and the phosphoamino acids determined on samples eluted from the chromatographs. Lyophilized peptides were dissolved in 6 N HCl (200 μl), heated at 105°C for 2 h, and lyophilized again. The hydrolysates were dissolved in H_2O containing 1 mg/ml each of P-serine, P-threonine, and P-tyrosine markers (Sigma Immunochemicals), applied to cellulose thin-layer sheets, and subjected to either ascending chromatography in isobutyric acid/0.5 M NH_4OH (5:3 vol/vol), or electrophoresis for 2 h at 750 V in the above acetic acid/formic acid buffer using silica gel plates. Phosphoamino acid spots detected by ninhydrin staining and autoradiography could also be cut out to determine the relative [^{32}P] content by liquid scintillation counting.

Analysis of Protein Phosphatase Activity

Cells grown in 16-mm wells were prelabeled with [^{32}P]phosphate, and then incubated with 400 nM calyculin A (LC Services Corp., Woburn, MA) at 37°C either alone, or before and after treatments with the various agents which induce MLC dephosphorylation. Incubation reactions were stopped by lysing cells at 2°C as described above, and the detergent-insoluble fractions were washed with CLB and prepared for gel electrophoresis by addition of SDS sample buffer.

To examine phosphatase activity in situ, cells were prelabeled with [^{32}P]phosphate, lysed, and the cytoskeletons incubated for 10 min at 30°C in 100 μl of 50 mM Tris-HCl, 50 mM NaCl, 5.0 mM $MgCl_2$, 1.5 mM PMSF, 1 mM DTT, pH 7.0. Reactions were terminated by addition of 4× CHES–SDS sample buffer, boiled, and subjected to 2-D gel electrophoresis.

Analysis of Protein Kinase Activity

Four confluent 35-mm dishes of thyroid cells were washed at 2°C with 20 mM Hepes, 1.5 mM PMSF, 5 mM $MgCl_2$, 1 mM DTT, pH 7.4 (kinase buffer). Cells were then collected with a rubber policeman in 2 ml of kinase buffer, homogenized by 10 passes with a Teflon-to-glass homogenizer, sonicated 15 s with a W-380 Heat Systems sonicator (Heat Systems–Ultrasonics, Inc., Farmingdale, NY) (80% output power), and further homogenized as above. Fractions were then made 0.1 mM $CaCl_2$, 5 mM EGTA, 50 μM W_7 (Rikaken Co. Ltd., Nagoya, Japan) or TFP (Sigma Immunochemicals), or 20 μM cAMP. Homogenate aliquots of 70 μl were incubated at 33°C with 10 μl of 4 mM [γ-^{32}P]ATP (200 cpm/pmol) (synthesized by the Molecular Endocrinology Core Laboratory of the Diabetes and Endocrinology Research Center of Baylor College of Medicine). After 3 min, reactions were terminated by addition of 4× CHES-SDS 2-D electrophoresis sample buffer and boiling. The same procedure was done using thyroid follicles isolated as described previously (37). The fibroblast samples were analyzed by 1-D electrophoresis. For analysis of protein kinase activity associated with the cytoskeletons, cells were lysed with 1% Triton X-100 in kinase buffer and then washed with kinase buffer alone at 2°C. The insoluble material on the dishes was then incubated for 3 min at 24°C in kinase buffer containing [γ-^{32}P]ATP and the above agents. Reactions were terminated by addition of 4× CHES–SDS sample buffer as above, and samples were subjected to 2-D gel electrophoresis.

Fluorescent Staining and Light Microscopy

Isolated thyroid follicles were grown on glass coverslips for 6–14 d to confluency in plastic petri dishes containing 6H Coon's media described above. Before experimentation, cells were incubated in 5H (-TSH) media for 1–2 d to achieve a basal, unstimulated condition. After this period, the various agents were added, and cells were further incubated for the indicated times. Coverslips were then removed, washed in PBS, and fixed for 5 min with 1% glutaraldehyde (Ted Pella, Inc., Redding, CA) in PBS at 25°C. Cells were permeabilized with 0.5% Triton X-100 in PBS for 10 min at 25°C, and autofluorescence quenched with 1 mg/ml sodium borohydride in PBS on ice. After blocking with 1% BSA, cells were incubated at 25°C for 30 min with rhodamine–phalloidin (Molecular Probes, Inc., Eugene, OR) diluted in blocking solution, washed in PBS, and coverslips were mounted on glass slides with PBS containing Airvol (Air Products & Chemicals, Inc., Allentown, PA). For localization of myosin, cells were first permeabilized at 2°C with 1% Triton as described above for phosphorylation studies. Coverslips were then immersed in −20°C methanol for 8 min to fix the detergent-insoluble cytoskeletal protein. After blocking with 1% BSA in PBS, coverslips were incubated overnight at 25°C with antibody against human platelet myosin (Biomedical Technology Inc., Stoughton, MA), followed by a 2-h incubation with rhodamine goat anti-rabbit IgG (Jackson ImmunoResearch Laboratories Inc., West Grove, PA). All cells were examined with a Zeiss Axiophot microscope, and photographs recorded on Tri-X Pan film (Eastman Kodak Co.).

Phase-Contrast Video Microscopy

The movement of cells was visualized using a Zeiss IM inverted microscope with a DAGE-72 camera interfaced with a Panasonic AG 6720 video recorder. Regions from a confluent monolayer of cells in 5H media were first recorded to assess unstimulated cell behavior. Cells were maintained at 37°C by fan heating and gassed with CO_2 to control pH of the media. After the addition of TPA to 0.2 μM, a field of cells was immediately selected, and typically recordings were done for 90 min. Printed images of cells at various time intervals were produced from the tape by a Sony UP-5000 video printer.

Scanning and Transmission EM and Analysis of Bead Ingestion

Thyroid cells cultured on glass coverslips were treated with a 0.04% suspension of 1 μm carboxylated latex beads (Polysciences Inc., Warrington, PA) and agents in 5H media at 37°C for 30 min. Cells were then washed several times with PBS, and fixed with 2.5% glutaraldehyde in 0.1 M cacodylate/0.2 M sucrose buffer, pH 7.2, for 1–2 h at 25°C. Samples were postfixed for 1 h in 1% OsO_4, dehydrated in graded ethanols, and critical point dried. Specimens were sputter coated with platinum, and examined with a CM-12 Philips electron microscope. Scanning EM micrographs were obtained in secondary and backscattered modes, and were digitized using a Synergy Framestore and Synoptics software on a PC. Images were printed with a Sony UP-5000 video printer.

The relative extent of latex bead ingestion induced by TSH and TPA was determined in cells prepared for transmission EM analysis of ultrastructure. Cells were plated in 60-mm Lux Permanox culture dishes (Electron Microscopy Sciences, Fort Washington, PA), and grown to confluency. Cells in 5H media for 1–2 d were then exposed to a 0.04% suspension of 1 μm carboxylated latex beads containing 40 mU/ml TSH, 0.2 μM TPA or no agent (control) for 30 min at 37°C. Surface beads were removed by washing several times with PBS, and cells were fixed in 2.5% glutaraldehyde in PBS for 2 h at 25°C. Cells were then postfixed in 1% OsO_4, dehydrated with graded ethanols, and embedded in Spurr's epoxy resin (Ted Pella, Inc.). For transmission EM analysis, 0.08-μm vertical sections were prepared, stained with Reynold's lead and uranyl acetate, mounted on formvar-coated copper slot grids, and examined with a Philips 410 electron microscope. Bead ingestion

was quantitated by preparing 1-μm-thick vertical sections which were then mounted on glass slides, and examined using phase contrast microscopy (100× objective) on a Zeiss Axiophot microscope. To increase the accuracy of determining the relative extent of bead ingestion by cells under various conditions, sections were cut 70 μm apart so that each cell region examined (usually 2,500 from each treatment) was from a different cell.

Results

Identification of Two Phosphorylated Myosin Light Chain Species by ATP Extraction and Antimyosin Immunoprecipitation

Previous analyses (26, 27) of cultured thyroid cell [^{32}P]-phosphoproteins associated with the Triton X-100 insoluble fraction revealed two proteins of 19 and 21 kD which appeared to be MLCs. To more definitively identify MLC, 2-D PAGE was used to analyze cytoskeletal fractions extracted with buffer containing ATP/KCl, which dissociates myosin from F-actin. After extraction, the majority of [^{32}P]phosphoproteins of 19 and 21 kD, pI 4.9–5.1, are present in the extract and not in the residual cytoskeletal fraction (data not shown). The extract was further subjected to immunoprecipitation using antiserum against thymus myosin. Fig. 1 shows a 2-D PAGE autoradiogram of the immunoprecipitate from the myosin extraction buffer fraction. Only two [^{32}P]phosphoproteins of 19 and 21 kD are observed in the immunoprecipitate, thus identifying these proteins as light chains of myosin. When one tenth of the antiserum was used for immunoprecipitation, the radioactive proteins were proportionally reduced (data not shown). The reason for the lesser amount of radioactivity associated with the 19-kD species is unknown since nearly equal radioactivity is observed when labeled cytoskeletons are immediately solubilized for electrophoresis.

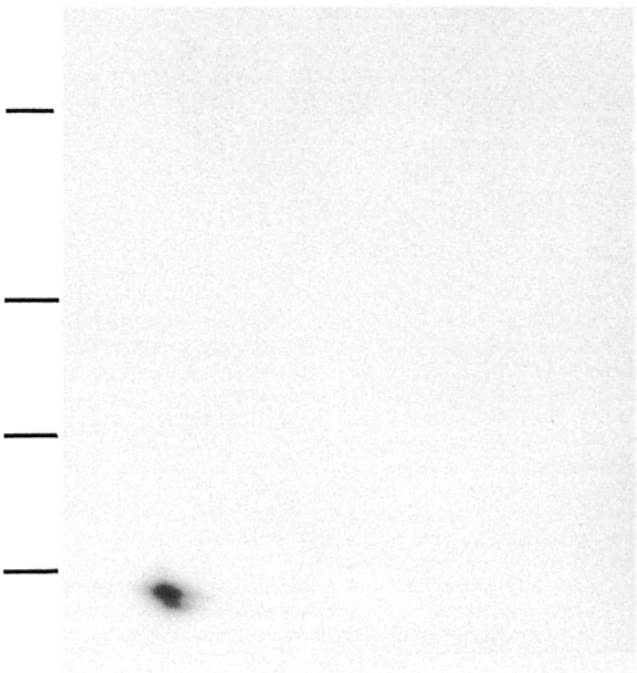

Figure 1. 2-D SDS-PAGE analysis of phosphoproteins immunoprecipitated with anti-thymus myosin serum. Cytoskeletons from [^{32}P]phosphate-labeled thyroid cells were extracted with myosin extraction buffer and the extracted material immunoprecipitated with antimyosin serum and subjected to 2-D PAGE (see Materials and Methods). Acidic pH region is left, basic pH region is right. Black bars on left, bottom to top represent 21.5-, 31-, 45-, and 66.2-kD molecular mass markers.

TSH and TPA Induce Dephosphorylation of Cytoskeletal MLC

Figs. 2, *A* and *B* are autoradiograms of cytoskeletal and cytosolic [^{32}P]phosphoproteins, respectively, prepared from control, "basal" thyroid cells. Greater than 90% of the radioactivity associated with the [^{32}P]phospho-MLCs (^{32}P-MLCs) is found in the detergent-insoluble cytoskeletal fraction. Previous determinations of intracellular [γ-^{32}P]ATP specific activity and stoichiometry of insoluble 19-kD/21-kD protein phosphorylation show that under basal conditions, this [^{32}P] radioactivity associated with MLC represents between 0.8–0.9 mol phosphate/mol light chain protein (26, 27). After treatment of intact, prelabeled cells with 40 mU/ml TSH for 20 min, the total ^{32}P-MLC radioactivity is reduced by >90% (Fig. 2, *C* and *D*). No ^{32}P-MLC is detected in the cytosolic fraction (Fig. 2 *D*), indicating a dephosphorylation reaction had occurred rather than dissociation of ^{32}P-MLC from the cytoskeleton. However, densitometric quantitation of myosin heavy chain from 1-D PAGE revealed that myosin associated with the insoluble fraction of TSH-treated cells decreased to 65 ± 5% (mean ± SEM, n = 4) of the amount found in control cells. The data indicate therefore that ~35% of the detergent-insoluble myosin containing predominantly dephosphorylated MLC becomes detergent soluble. In addition to P-MLC, two basic (pI 7–8) major cytosolic phosphoproteins (20 kD) of unknown identity (Fig. 2 *B*, *bracket*) are dramatically dephosphorylated after TSH treatment (Fig. 2 *D*). This concentration of hormone was used since it increases intracellular cAMP to near maximal levels (37). MLC is similarly dephosphorylated by treatment of cells with 1 mM dibutyryl cAMP (data not shown).

After treatment of prelabeled cells with 0.2 μM TPA for 20 min, the total ^{32}P-MLC radioactivity is reduced by ~60% (Fig. 2, *E* and *F*), while other proteins of higher molecular weight are phosphorylated to a greater extent than controls. TPA treatment, like TSH, reduced further the ^{32}P-MLC radioactivity in the cytosolic fraction (Fig. 2 *F*) compared with control, which is also consistent with net MLC dephosphorylation. Quantitation of detergent-insoluble myosin heavy chain also showed that cytoskeletal myosin was reduced to 86 ± 12% (mean ± SEM, n = 4) of control cell myosin; the lesser degree of myosin "solubilization" compared with that observed with TSH treatment could correlate with the differences in extent of MLC dephosphorylation. The two basic, cytosolic 20-kD proteins are also dephosphorylated after TPA treatment (Fig. 2 *F*), although as for P-MLC, the reduction is not as great as that caused by TSH. The dose of TPA used was maximal for effects on phosphorylation, since results were the same at concentrations up to 1 μM; the inactive 4 α-phorbol analog of TPA was without effect.

Agonist-Induced MLC Dephosphorylation Is Regulated at the Protein Phosphatase Level

Decreases in the MLC phosphorylation state induced by agents shown in Fig. 2 could result from inhibition of kinase

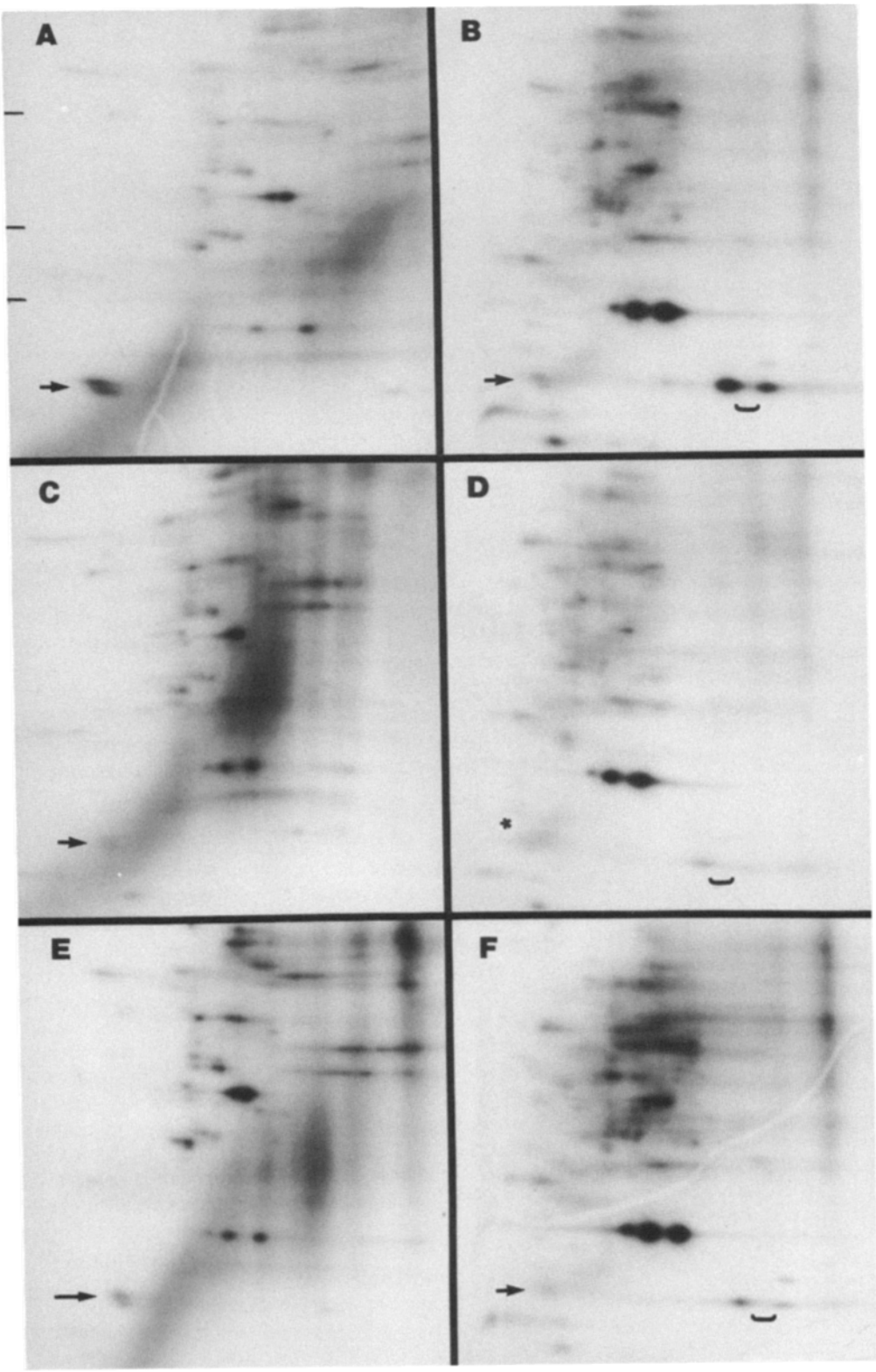

Figure 2. 2-D SDS-PAGE analysis of cytoskeletal and cytosolic phosphoproteins from thyroid cells treated without or with TSH or TPA. Cells prelabeled with [^{32}P]-phosphate were incubated for 20 min without (*A* and *B*) or with 40 mU/ml TSH (*C* and *D*) or 0.2 μM TPA (*E* and *F*) and the cytoskeletal (*A*, *C*, and *E*) and cytosolic (*B*, *D*, and *F*) fractions, prepared by lysis, were subjected to 2-D PAGE (see Materials and Methods). Arrows point to 19- and 21-kD phosphomyosin light chains. Brackets point to 20-kD cytosolic phosphoproteins. Below asterisk is 21-kD region. Black bars on left side of *A* represent, bottom to top, 31-, 45-, and 66.2-kD molecular mass markers.

or stimulation of phosphatase activity. The enzymic pathway for net MLC dephosphorylation was examined using the potent phosphatase 1 and 2A inhibitor, calyculin A. After treatment of prelabeled cells with 40 mU/ml TSH for 10 min, insoluble ^{32}P-MLC radioactivity is reduced by ~50% (Fig. 3 *B*) compared with control (Fig. 3 *A*). When TSH-treated cells are incubated for an additional 10 min at 400 nM calyculin A, insoluble ^{32}P-MLC radioactivity is increased 3.5-fold (Fig. 3 *C*) compared with control; Fig. 3 *D* shows the decreased ^{32}P-MLC after 20 min in TSH alone. Treatment of cells with calyculin A alone for 20 min results in a similar increased insoluble ^{32}P-MLC radioactivity and ac-

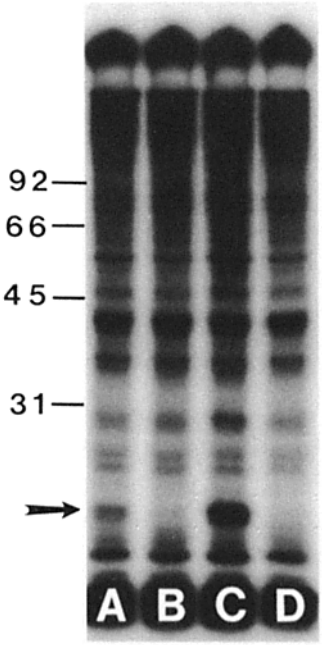

Figure 3. 1-D SDS-PAGE analysis of cytoskeletal phosphoproteins from thyroid cells treated without or with TSH and calyculin A. Cells prelabeled with [^{32}P]phosphate were incubated for 20 min without (*A*) or with 40 mU/ml TSH for 10 min (*B*), 10 min with TSH and 10 min with 400 nM calyculin A (*C*), or 20 min with TSH (*D*). Cytoskeletal fractions were then prepared by lysis, and subjected to 11.5% 1-D PAGE/autoradiography (see Materials and Methods). Arrow points to 19- and 21-kD phosphomyosin light chains. Black bars on left side represent 31-, 45-, 66-, and 92-kD molecular mass regions.

tomyosin contraction determined by rhodamine-phalloidin staining (data not shown). Since MLC is hyperphosphorylated upon phosphatase inhibition in the presence as well as in the absence of TSH, the agonist-induced dephosphorylation process appears to be operating via phosphatase stimulation and not kinase inhibition. These results are also observed with dbcAMP and TPA treatments (data not shown).

A close spatial relationship of a phosphatase with MLC could facilitate regulation of the phosphorylation state. Such association was examined by incubating [^{32}P]phosphoproteins of the detergent-insoluble cytoskeletal fraction from prelabeled, unstimulated, basal cells in buffer potentially conducive to phosphatase activity (50 mM Tris, 50 mM NaCl, 1 mM DTT, 5 mM $MgCl_2$, 1 mM EGTA, 1.5 mM PMSF, pH 7.0). After a 10 min incubation in this buffer at 30°C, ^{32}P-MLC is dephosphorylated by 95%, and although the [^{32}P]phosphate content of several other proteins is also reduced, most phosphoproteins are not dephosphorylated as extensively as MLC under these conditions (data not shown). Inclusion of 20 μM cAMP, 0.1 mM ATP, and 75 μg/ml purified A-kinase did not enhance dephosphorylation of MLC at shorter incubations periods when the extent of dephosphorylation was less than that achieved after longer incubations.

Analysis of Phosphoamino Acid Sites of MLCs

The phosphorylation pattern of MLC isoforms seen in Figs. 1 and 2 is not limited to a single pI value, similar to that observed for platelet MLC (28). Therefore, either multiple sites containing residues of a particular amino acid are phosphorylated and/or different types of amino acids are phosphorylated. Table I shows that in untreated, basal thyroid cells, MLC associated with the detergent-insoluble cytoskeletal fraction is phosphorylated at predominantly threonine and serine residues, although phosphotyrosine is detected to a minor extent. Treatment of intact cells with 40 mU/ml TSH (as also seen in Fig. 2 *C*) dramatically reduces phosphorylation of cytoskeletal MLC resulting in almost undetectable levels of phosphoamino acids (Table I) which is also observed after in vitro dephosphorylation of ^{32}P-MLC associated with detergent-insoluble cytoskeletal preparations. Treatment with 0.2 μM TPA (as also seen in Fig. 2 *E*) results in a 56 ± 19% reduction in cytoskeletal ^{32}P-MLC, with little change in the relative proportions of phosphoamino acids compared to control conditions (Table I).

Table I. Phosphoamino Acid Analysis of Cultured Dog Thyroid Cell MLC

Treatment	Percent P-threonine	Percent P-serine	Percent P-tyrosine	Percent MLC dephosphorylation
Control*	61 ± 4	34 ± 3	5 ± 5	–
TSH (40 mU/ml)‡	N.D.	N.D.	N.D.	>95
TPA (0.2 μM)§	59 ± 8	33 ± 1	8 ± 8	56 ± 19

Cytoskeletal fractions from [^{32}P]phosphate-labeled cells treated with or without TSH or TPA were subjected to 2-D PAGE. The ^{32}P-MLC regions in the gels were excised and the ^{32}P-amino acids from the hydrolysates were analyzed as described in Materials and Methods. Values for percentage ^{32}P-amino acid and dephosphorylation of ^{32}P-MLC are the mean ± standard deviation.
* Five separate experimental determinations.
‡ Two determinations.
§ Three determinations.
N.D., not determined.

2-D mapping of tryptic phosphopeptides of both smooth muscle and nonmuscle MLC can distinctly resolve the highly conserved peptides containing C-kinase phosphorylation sites from the peptide containing the MLCK site at serine 19 (28). Fig. 4, *A* and *B* show phosphopeptide maps of the 21- and 19-kD ^{32}P-MLC tryptic digests, respectively, from basal cells. Both MLC species have similar phosphopeptide patterns composed of three labeled peptides. The major radioactive peptide, indicated by the open arrow, migrates furthest upon electrophoresis, relatively little upon chromatography, and contains both phosphothreonine and phosphoserine residues (Fig. 4 *D*, lanes *1* and *2*). Considering the conserved amino acid sequences of phosphorylated MLC tryptic digests, this peptide corresponds to that containing phosphothreonine 18 and phosphoserine 19. The minor phosphopeptide above the major spot corresponds to the peptide containing a site(s) phosphorylated by purified C-kinase in vitro (not shown), and is reported to contain phosphoserine 1 or 2 (28). Radioactivity near the origin represents the same tryptic fragment phosphorylated at both serine 1 and 2 which is also observed after in vitro phosphorylation of myosin by C-kinase. It should be noted here that peptide maps of ^{32}P-MLC tryptic digests from TPA-treated cells showed a decrease in all labeled peptides indicating that TPA did not decrease phosphorylation at one or more sites and concomitantly increase phosphorylation at a C-kinase site(s) (data not shown). Fig. 4 *C* shows the map of tryptic phosphopeptides of the 21-kD MLC after hyperphosphorylation induced by the phosphatase inhibitor, calyculin A, shown in Fig. 3. As could be predicted, phosphorylation at serine 1 or 2 alone is no longer apparent, and a concomitant increase in the peptide containing phosphoserine 1 and 2 is evident near the origin. Also present is the phosphothreonine/phosphoserine-containing peptide (Fig. 4, *open arrows*) as well as a new phosphopeptide to the extreme right (Fig. 4, *solid arrow*) containing only phos-

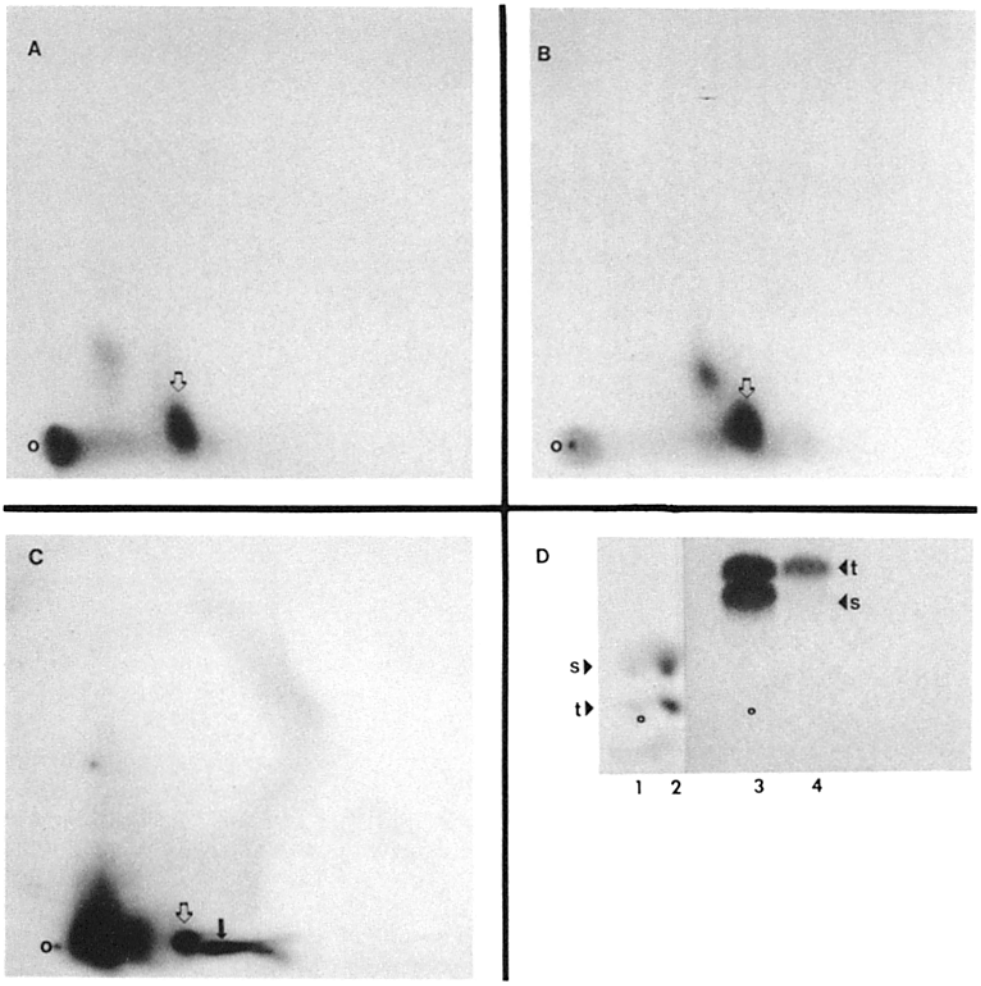

Figure 4. 2-D phosphopeptide mapping and phosphoamino acid analyses of 21- and 19-kD MLC tryptic digests. ^{32}P-MLC from detergent-insoluble cell fractions was isolated by 2-D gel electrophoresis. The 21- and 19-kD proteins were cut from the gel, digested with trypsin, and phosphopeptides resolved by electrophoresis (left to right) followed by chromatography (bottom to top) or thin layer cellulose plates. Origin is indicated by (o). *A* and *B* show autoradiograms of ^{32}P-peptides from 21- and 19-kD MLC of control basal cells, respectively. *C* shows tryptic ^{32}P-peptides of the 21-kD MLC from cells treated with calyculin A. Autoradiography in *C* is quantitatively reduced relative to *A* and *B* to show spot resolution. Open arrows point to the radioactive spot containing both phosphothreonine (*t*) and phosphoserine (*s*), amino acids which were resolved by electrophoresis (*D*, lanes *1* and *2*); solid arrow in *C* points to spot containing only phosphothreonine which was resolved by chromatography (*D*, lanes *3* and *4*). In *D*, lanes *1* and *3* show ninhydrin staining, and lanes *2* and *4* show autoradiography.

phothreonine (Fig. 4 *D*, lanes *3* and *4*). This additional site likely represents phosphorylation at threonine 9 since a similar spot is observed upon in vitro phosphorylation of MLC by C-kinase; however, without sequence data, phosphorylation at threonine 9 and/or 10 cannot be ruled out at this time.

Phosphorylation of MLC in Cultured Dog Thyroid Cells Is Ca^{2+}/Calmodulin Independent

Since MLC is phosphorylated in most systems studied by a specific Ca^{2+}/calmodulin-dependent kinase, the effect of various agents known to inhibit this enzyme by interfering with calmodulin was studied. Fig. 5 shows 2-D PAGE autoradiograms of cultured dog thyroid cell homogenate proteins phosphorylated with 0.5 mM [γ-^{32}P]ATP for 3 min at 33°C. In the presence of 0.1 mM $CaCl_2$ (Fig. 5 *A*), the MLCs are significantly phosphorylated, and the addition of either 5 mM EGTA (Fig. 5 *B*), 50 μM W_7 (Fig. 5 *C*) or 50 μM W_7/5 mM EGTA (Fig. 5 *D*) has no inhibitory effect on the extent of MLC phosphorylation. The same result is obtained using trifluoperazine (TFP) rather than W_7 to inhibit calmodulin, or using homogenates of freshly prepared dog thyroid follicles (data not shown). In addition, the presence of 20 μM cAMP alone or together with 75 μg/ml purified A-kinase had no effect on the phosphorylation of MLC, although the phosphorylation of some other proteins was enhanced (data not shown).

Since a Ca^{2+}/calmodulin-dependent kinase has been shown to phosphorylate MLC in cultured fibroblasts, homogenates of dog thyroid fibroblasts were used as an internal comparison. Fig. 6 shows a 1-D PAGE autoradiogram of fibroblast homogenate proteins phosphorylated as above. In the presence of 0.1 mM $CaCl_2$ a 20-kD protein is significantly phosphorylated (Fig. 6 *a*), whereas 5 mM EGTA (Fig. 6 *b*) or 50 μM TFP (Fig. 6 *c*) inhibits phosphorylation by 90 and 75%, respectively. Phosphorylation of an ~94-kD protein (Fig. 6, *small arrow*) is also inhibited by these agents.

Association of Kinase Activity with the Cytoskeleton

Protein kinase activity and phosphorylated substrates associated with the detergent-insoluble fraction were examined and compared using bovine and dog thyroid cells. Unstimulated, basal cells were lysed, briefly washed with 20 mM Hepes, 0.1 mM $CaCl_2$, 5 mM $MgCl_2$, 1 mM DTT, 1 μg/ml antipain, 1 μg/ml leupeptin, 1.5 mM PMSF, pH 7.6 (kinase buffer) at 2°C, and then incubated in this buffer containing 0.5 mM [γ-^{32}P]ATP for 3 min at 24°C. Fig. 7 *A* shows a

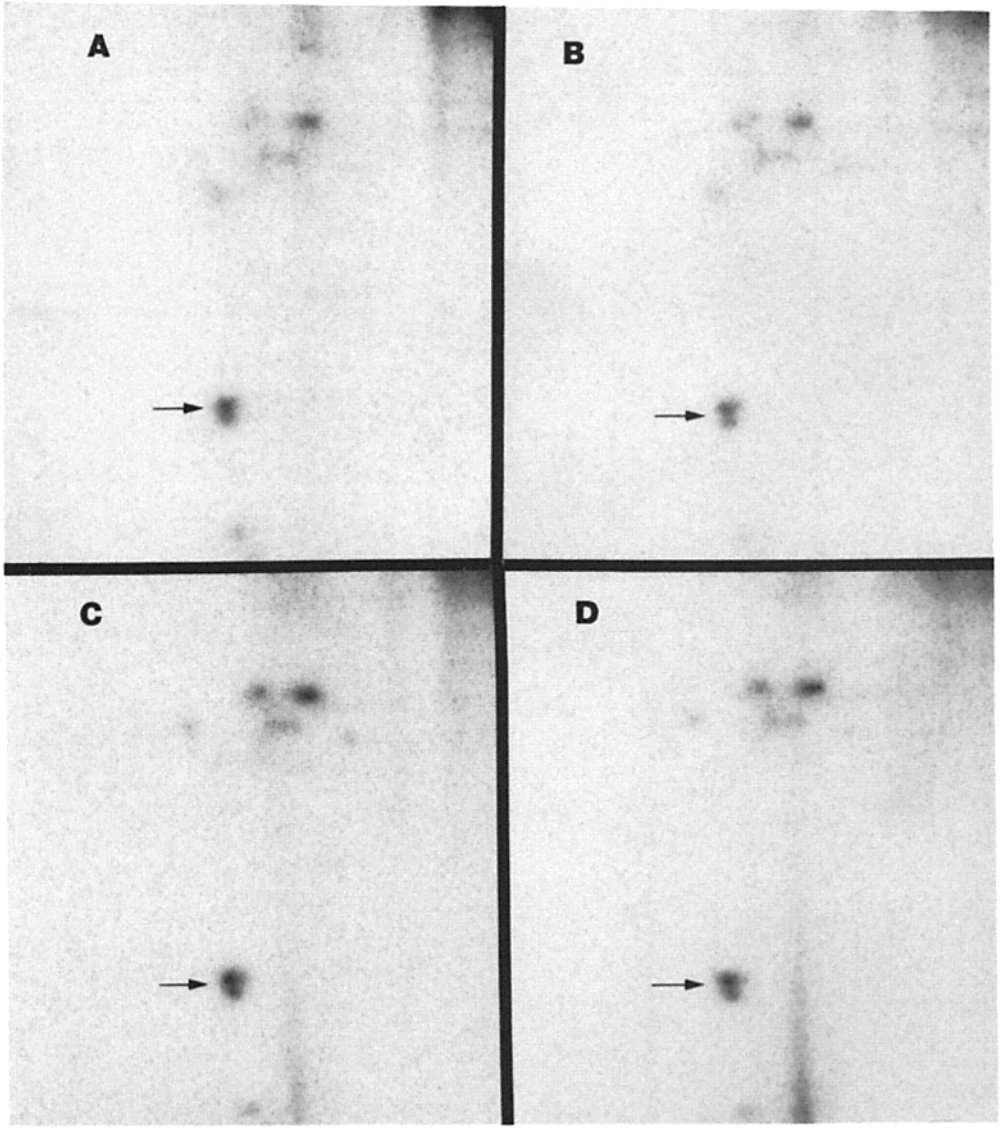

Figure 5. 2-D SDS-PAGE analysis of thyroid cell homogenate proteins phosphorylated with [γ-^{32}P]ATP. Homogenates of cultured thyroid cells were prepared in 20 mM Hepes, 5 mM $MgCl_2$, 1 mM DTT, 1.5 mM PMSF, pH 7.4 (kinase buffer) as described in Materials and Methods. Aliquots containing 0.1 mM $CaCl_2$ (*A*), 5 mM EGTA (*B*), 50 μM W_7 (*C*), or 50 μM W_7 and 5 mM EGTA (*D*) were then incubated with 0.5 mM (γ-^{32}P]ATP (200 cpm/pmol) for 3 min at 33°C. Samples were then prepared for 2-D PAGE. Arrows point to phosphomyosin light chains.

2-D PAGE autoradiogram of phosphorylated bovine detergent-insoluble proteins, of which is a single 20-kD protein with a pI value similar to dog MLC. Likewise, dog cytoskeletal MLC is phosphorylated (Fig. 7 *B*), however, unlike that of bovine thyroid cells, P-MLC is the dominant phosphoprotein and consists of 19- and 21-kD species.

MLC Dephosphorylation Is Accompanied by Stress Fiber Disruption

Basal cells cultured in the absence of TSH contain two spatially distinct, well-developed actin stress fiber complexes representing much of the detergent-insoluble actin. Fig. 8 *A* shows rhodamine (rh)-phalloidin staining of dorsal stress fibers (Fig. 8 *A*, arrow) which stretch across the cells in a parallel fashion. The zonulae adherens, typical of cultured epithelial cells, are also clearly stained with the fluorescent label. Fig. 8 *B* shows rh-phalloidin staining of thicker ventral stress fiber bundles which appear to radiate from focal adhesion plaques located in cell-substratum contact regions. After treating cells with 40 mU/ml TSH for 30 min, which causes almost complete MLC dephosphorylation (Fig. 2, *C* and *D*), both the dorsal (Fig. 8 *C*) and ventral (Fig. 8 *D*) stress fiber complexes are disrupted as determined by undetectable filamentous rh-phalloidin staining. Staining of the zonulae adherens is not affected by hormone treatment, suggesting that the F-actin population of this region is resistant to the disassembly process. In addition, numerous punctate, rod-like structures stain throughout the dorsal cell surface (Fig. 8 *C*), and appear to correlate with disassembly resistant F-actin of microvilli and pseudopods. Cell processes which frequently extend from ventral regions after TSH or dbcAMP treatment (Fig. 8 *D*) also stain rather strongly with rh-phalloidin (Fig. 8 *D*, *black arrows*).

Although TPA treatment causes dissolution of stress fiber structure per se (Fig. 8, *E* and *F*), F-actin bundles persist in the presence of this agent, which could correlate with the lesser extent of MLC dephosphorylation compared to TSH treatment (Fig. 2). After treating cells with 0.2 μM TPA for 30 min, dorsal stress fibers are disrupted (Fig. 8 *E*), although a few occasionally remain (Fig. 8 *E*, *white arrowheads*). Fig. 8 *F* shows the ventral cell region where stress

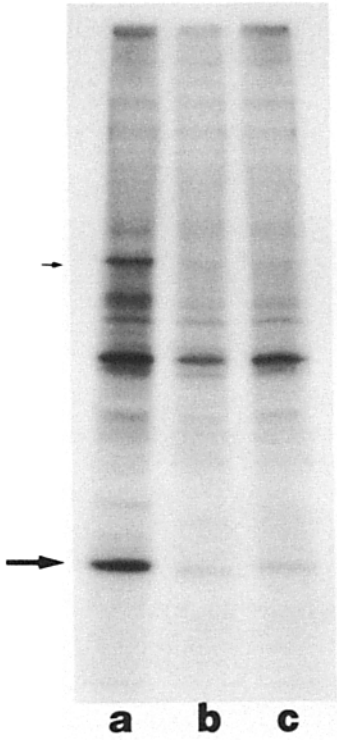

Figure 6. 1-D SDS-PAGE analysis of thyroid fibroblast cell homogenate proteins phosphorylated with [γ-^{32}P]ATP. Homogenates of cultured thyroid fibroblasts cells were prepared in 20 mM Hepes, 5 mM $MgCl_2$, 1 mM DTT, 1.5 mM PMSF, pH 7.4 (kinase buffer) as described in Materials and Methods. Aliquots containing 0.1 mM $CaCl_2$ (*a*), 5 mM EGTA (*b*), or 50 μM TFP (*c*) were incubated with 0.5 mM [γ-^{32}P]ATP (200 cpm/pmol) for 3 min at 33°C. Samples were then prepared for 1-D PAGE. Large and small arrow points to 20- and 94-kD phosphoprotein, respectively.

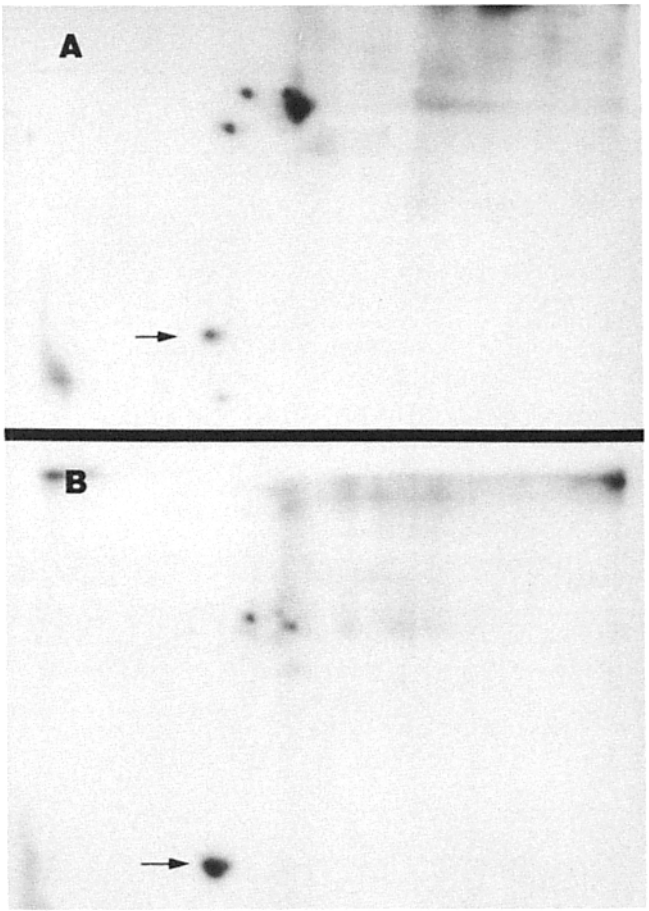

Figure 7. 2-D SDS-PAGE analysis of bovine and canine thyroid cell cytoskeletal proteins phosphorylated with [γ-^{32}P]ATP. Cultured bovine (*A*) or canine (*B*) thyroid cells were lysed and cytoskeletons washed with 20 mM Hepes, 5 mM $MgCl_2$, 1 mM DTT, 1.5 mM PMSF, pH 7.4 (kinase buffer) at 2°C as described in Materials and Methods. Cytoskeletons were incubated in kinase buffer containing 0.1 mM $CaCl_2$ and 0.5 mM [γ-^{32}P]ATP (200 cpm/pmol) for 3 min at 24°C. Samples were then prepared for 2-D PAGE. Arrows point to 20-kD phosphomyosin light chain (*A*), and 21- and 19-kD phosphomyosin light chains (*B*).

fibers appear to have rearranged and condensed forming large swirls of F-actin bundles that stain intensely with rh-phalloidin (Fig. 8 *F, black arrowheads*); sheets of F-actin which resemble lamellipodia, are also observed in this region.

The distorted, asymmetric patterns of ventral F-actin staining observed after TPA treatment accompany an increased protrusive and motile behavior of cells (Fig. 9). Furthermore, rh-phalloidin staining of zonulae adherens F-actin appears to be significantly reduced by TPA treatment compared to basal and TSH-treated cells (Fig. 8). Fig. 9 shows frames from video microscopy of live cells after 0.2 μM TPA treatment. Significant changes in cell shape and orientation can be observed for most cells in the selected field, although in particular, note the four cells within the 140 × 80 μm boxed area. Perhaps the most dramatic changes occur during the first 20 min after TPA addition (Fig. 9 *b*), when cells retract and begin protruding. Dorsal cell membrane regions can also be found to bleb and ruffle which probably correlates with stress fiber disruption in this vicinity. Even after 80 min (Fig 9 *e*), cells continue to reorient with respect to their neighbors. Note particularly the cell indicated by the black arrow which expands and extends from a horizontally elongated to vertical position (Fig. 9, *a–e*).

TSH and TPA Induce a Reorganization of Cytoskeletal Myosin After Stress Fiber Disruption

As shown in Fig. 2, *A* and *B*, most of the phosphorylated MLC is associated with the detergent-insoluble fraction in basal cells. Indirect immunofluorescence of this fraction with antimyosin reveals that myosin is localized on both dorsal and ventral stress fibers (Fig. 10 *A*) since the staining pattern reflects that observed with rh-phalloidin shown in Fig. 8, *A* and *B*. After a 30-min treatment of cells with 40 mU/ml TSH, antimyosin staining of stress fiber complexes is not observed, consistent with stress fiber disruption shown in Fig. 8, *C* and *D*. However, myosin appears to reorganize and associate with a fine, detergent-insoluble filamentous network throughout the cytoplasm (Fig. 10 *B*). In Fig. 10 *C*, after a 30-min treatment with 0.2 μM TPA, antimyosin also stains a filamentous network in many cells which appears similar to that observed after TSH treatment. Furthermore, after TPA treatment, a redistribution of myosin also appears to parallel that of F-actin in the ventral region shown in Fig. 8 *D*; myosin is associated with fine filamentous sheets as well as large, twisted bundles (Fig. 10 *C*, *open arrows*) in this cell region.

TSH, but not TPA, Induces Phagocytosis of Latex Beads

The phagocytotic capacity of cultured thyroid cells in the presence of 1 μm carboxylate-modified latex beads was ex-

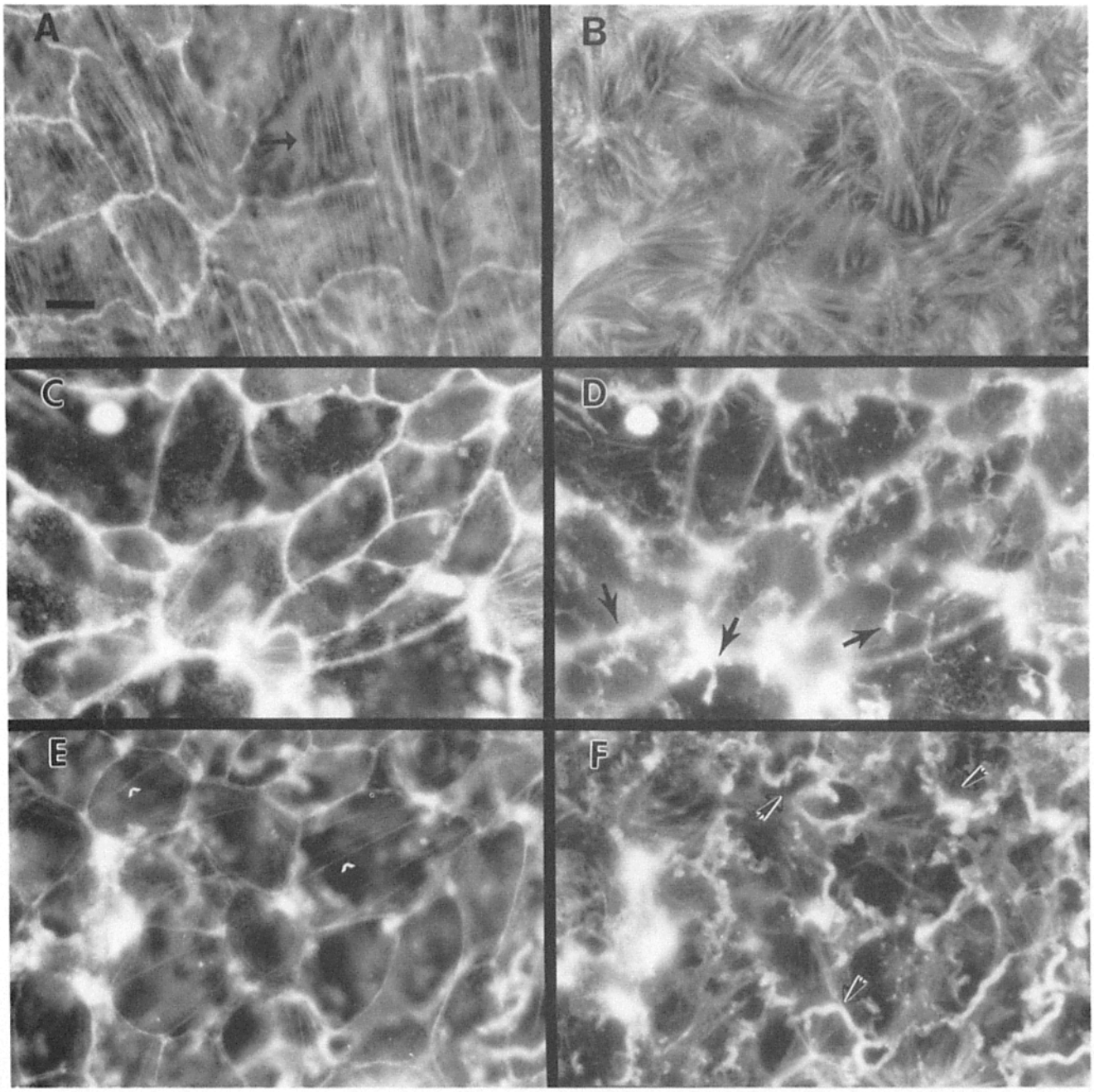

Figure 8. Rh-phalloidin staining of F-actin in cultured thyroid cells. Cells in 5H media alone (control) (*A* and *B*), were either incubated with 40 mU/ml TSH (*C* and *D*), or 0.2 μM TPA (*E* and *F*) for 30 min at 37°C. After treatment, cells were fixed, lysed, and stained with rh-phalloidin as described in Materials and Methods. In *A*, *C*, and *E* the microscope was focused on the dorsal cell region; in *B*, *D*, and *F*, focus was on the ventral region. Black arrow in *A* points to some dorsal stress fibers of untreated, control cells; TSH treatment abolished dorsal (*C*) and ventral (*D*) stress fibers, while the black arrows in (*D*) point to concentrated actin staining within extended ventral cell processes. White arrowheads in (*E*) point to a few remaining dorsal stress fibers after TPA treatment, while the black arrowheads in (*F*) point to some of the ventral actin ribbon-like structures. Bar, 10 μm.

amined after 30-min treatments without and with 0.2 μM TPA or 40 mU/ml TSH. By scanning EM, control cultures revealed an intact monolayer of predominantly flat cells with a variable density of small microvilli (Fig. 11, *A*). Occasionally, small ruffles and pseudopodial protrusions were observed on some cells. Upon TPA treatment Fig. 11 *B*), the cells rapidly retracted from their neighbors, became elongated, and extended over and under each other as also indicated by video microscopy (Fig. 9). A gross spatial reorganization or migration of cells is depicted in Fig. 9 *B*. Typically, the dorsal surfaces were ruffled and elevated, and large knobby protrusions were apparent at the cell periphery; microvilli number and density appeared similar to those of control cells. TSH-treated cells (Fig. 11, *C–F*), in contrast

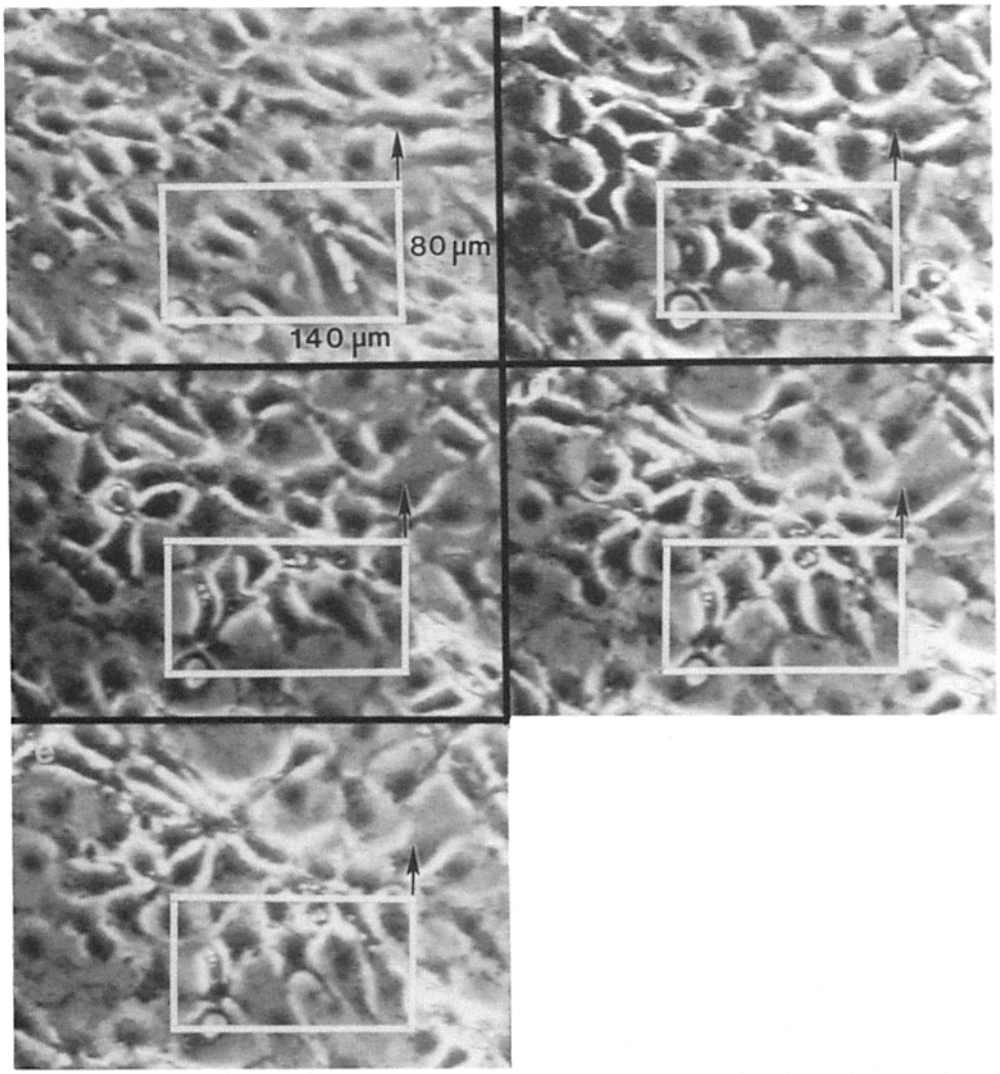

Figure 9. Phase-contrast video microscopy of thyroid cell shape changes and motility induced by TPA. A confluent cell monolayer in 5H media was treated at 37°C with 0.2 μM TPA; a field was immediately selected and recorded by video microscopy. Images shown were produced from the tape by a video printer at 1.5 (*a*), 20 (*b*), 40 (*c*), 60 (*d*), and 80 (*e*) min after TPA addition. Constant 140 × 80 μm areas (*white boxes*) were marked as a reference and contain four particularly active cells; black arrow in upper right corners points to a cell undergoing reorientation.

to TPA, developed a more rounded rather than elongated morphology, and retracted less frequently from their neighbors. Smooth-surfaced pseudopodial protrusions and ruffles were seen extending from the central regions and lateral margins (Fig. 11, *E* and *F*). Latex beads, shown in Fig. 11, *C* and *D* (*black arrow*), were commonly associated with these structures (Fig. 11, *C* and *D*, *white arrowheads*) which are probably the main sites of phagocytosis.

Fig. 12 *A* shows a transmission EM micrograph of a vertical section through a basal cell subjected to latex beads for 30 min at 37°C. Microvilli are present on the dorsal surface (Fig. 12 *A*, *arrowhead*). The section shows a prominent bundle of F-actin running horizontally beneath the dorsal surface, corroborating the pattern seen in cells stained with rh-phalloidin (Fig. 8 *A*). Periodic densely stained foci within the filaments (Fig. 8 *A*, *open arrows*) are present which are likely to be sites of F-actin bundling proteins such as α-actinin; filamin and myosin are probably located in between the foci (32). Quantitation of vertical, 1-μm-thick sections of cells (cell region) and intracellular beads therein by light microscopy (Fig. 13) shows that 6% of cell regions examined contained beads; only a few regions had more than four beads, and there were a couple above 8. However, after stimulating cells for 30 min with 40 mU/ml TSH (Fig. 12 *B*), the number of microvilli per surface area appeared to increase, pseudopods and complex phagocytic structures were observed (Fig. 12 *B*, *open arrow*), and 19% of cell regions examined contained significantly more beads (up to 25 per region) than controls (Fig. 13). Stress fiber bundles were not observed by EM under this condition, which corroborated their absence using rh-phalloidin (Fig. 8, *B* and *C*). While treating cells with 0.2 μM TPA for 30 min also caused dorsal stress fiber disruption and surface ruffles, it did not promote pseudopod formation (Fig. 12 *C*), and only 9% of the cell regions contained beads; relatively few regions had more than eight beads (Fig. 13). The small increase in bead uptake versus control could be due to bead entrapment and subsequent ingestion by the ruffled dorsal cell surface shown in Fig. 11 *B*. Microvilli at the dorsal surface (Fig. 12, *A* and *C*, *black arrowheads*) were similar to those of untreated control cells, and bundles of F-actin could be seen parallel to the ventral plasma membrane (*open arrows*).

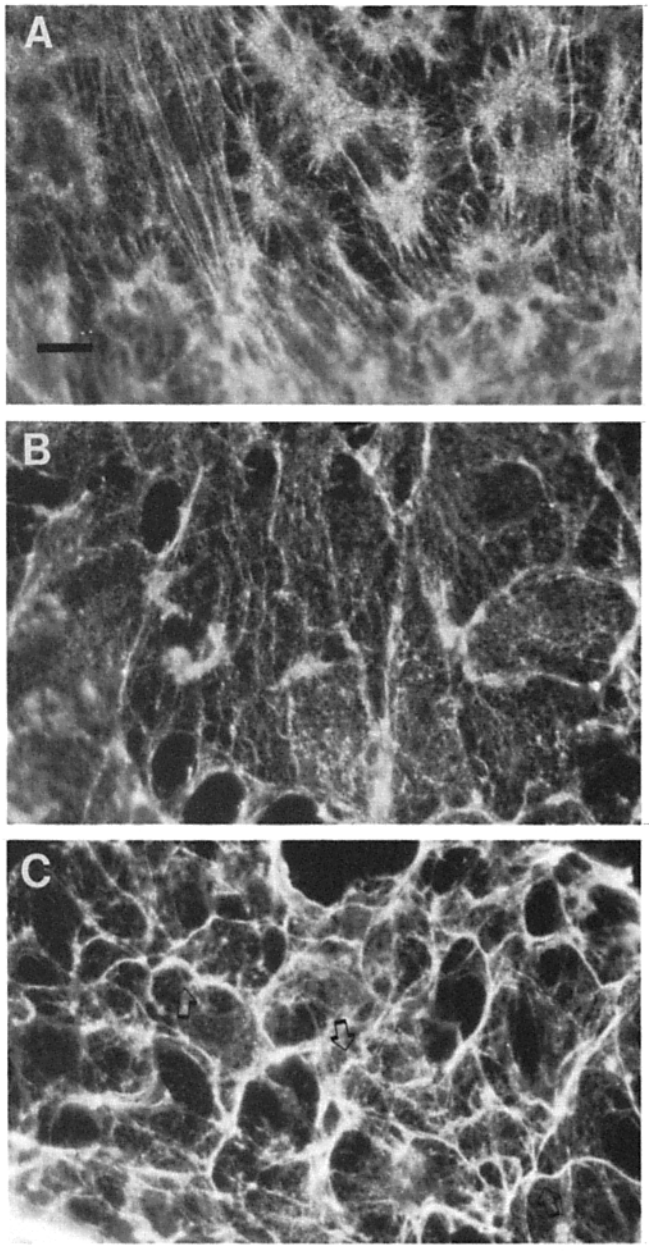

Figure 10. Immunofluorescent localization of detergent-insoluble myosin in cultured thyroid cells. Cells in 5H media alone (control) (*A*), were either incubated with 40 mU/ml TSH (*B*), or 0.2 μM TPA (*C*) for 30 min at 37°C. After treatment, cells were lysed, fixed, and stained with myosin antibody and rh-conjugated second antibody as described in Materials and Methods. In untreated basal cells (*A*), myosin localizes on parallel, dorsal stress fibers and radiating ventral bundles; TSH (*B*) and TPA (*C*) induce a rearrangement of this staining pattern. Open arrows in *C* point to myosin antibody staining of some twisting ribbon-like structures which also stain with Rd-phalloidin (see Fig. 8 *F*) in the ventral cell region. Bar, 10 μm.

Discussion

This study has identified 19- and 21-kD species of MLC which are phosphorylated at both threonine and serine residues by a Ca^{2+}-independent kinase(s) associated with the detergent-insoluble cell fraction of primary thyroid cell cultures from dog. Based on tryptic peptide/phosphoamino acid analyses, much of the phosphorylation corresponds to the threonine and serine sites phosphorylated by Ca^{2+}/calmodulin-dependent MLCK. Treatment of cells with TSH, dbcAMP or the phorbol ester, TPA, decreases the phosphorylation state of MLC which can be blocked and reversed by the phosphatase inhibitor, calyculin A. Relatively specific phosphatase activity for MLC is also associated with the insoluble, cytoskeletal fraction. There is a correlation between MLC dephosphorylation, the disruption of stress fibers, and the subsequent development of a different actomyosin network following either TSH or TPA treatment of cells. Although both agents apparently induce a reorganization of F-actin and myosin II upon disruption of stress fibers in the dorsal cell region, phagocytosis of latex beads in this cell region is induced primarily by TSH through a cAMP-mediated pathway.

MLC in the cultured thyroid cells, identified by antimyosin immunoprecipitates, is in a phosphorylated state, and is associated with the Triton X-100–insoluble cytoskeletal fraction under resting, basal conditions, which contrasts myosin II of other nonmuscle cells such as platelets (17). In unstimulated platelets, >90% of the MLC is detergent soluble and is not phosphorylated. Elevation of intracellular Ca^{2+} by the agonist, thrombin, or ionophore induces MLC phosphorylation via Ca^{2+}/calmodulin-dependent MLCK, and thus promotes the formation of "activated" actomyosin complexes, which participate in cell contraction and secretion. Stimulation of thyroid cells by the agonist, TSH, on the other hand, increases intracellular cAMP, which induces disruption of F-actin bundles and consequent changes in cell shape (37, 41, 52, 55); under these conditions MLC dephosphorylation is observed. These effects are reproduced by cAMP analogs, implicating an A-kinase mediated process. MLC dephosphorylation induced by cAMP in fibroblasts is also correlated with disruption of stress fibers and cell rounding (33). It is interesting in thyroid cells, that subsequent to dephosphorylation of MLC and stress fiber disruption, determined by rhodamine–phalloidin fluorescence, much of the myosin (and actin) remain detergent-insoluble (~55–75%) as determined from one dimensional PAGE analysis. Indirect immunofluorescence with myosin antibody reveals a fine filamentous network throughout the cytoplasm, suggesting that cAMP mediates a reorganization rather than extensive dissolution of actomyosin complexes.

The protein kinase C–stimulating phorbol ester, TPA, also induces thyroid MLC dephosphorylation (~60%) and stress fiber disruption, however, this agent does not reproduce TSH or dibutyryl cAMP effects on cell morphology and F-actin reorganization. Similar to that observed following TSH-treatment, most (>70%) of the actomyosin remains detergent-insoluble after TPA treatment. This is corroborated by the organization of F-actin into thick ribbon-like structures and sheets predominantly located in the ventral cell region, also observed in other cultured epithelial cells (29, 41, 44). These aggregates stain with antimyosin, and could contain the MLC fraction which is not dephosphorylated by TPA treatment. While TPA-induced phosphorylation of MLC has been implicated in C-kinase mediated platelet activation (2, 28), there is no evidence for such phosphorylation in this thyroid cell system. It is plausible that these prominent ven-

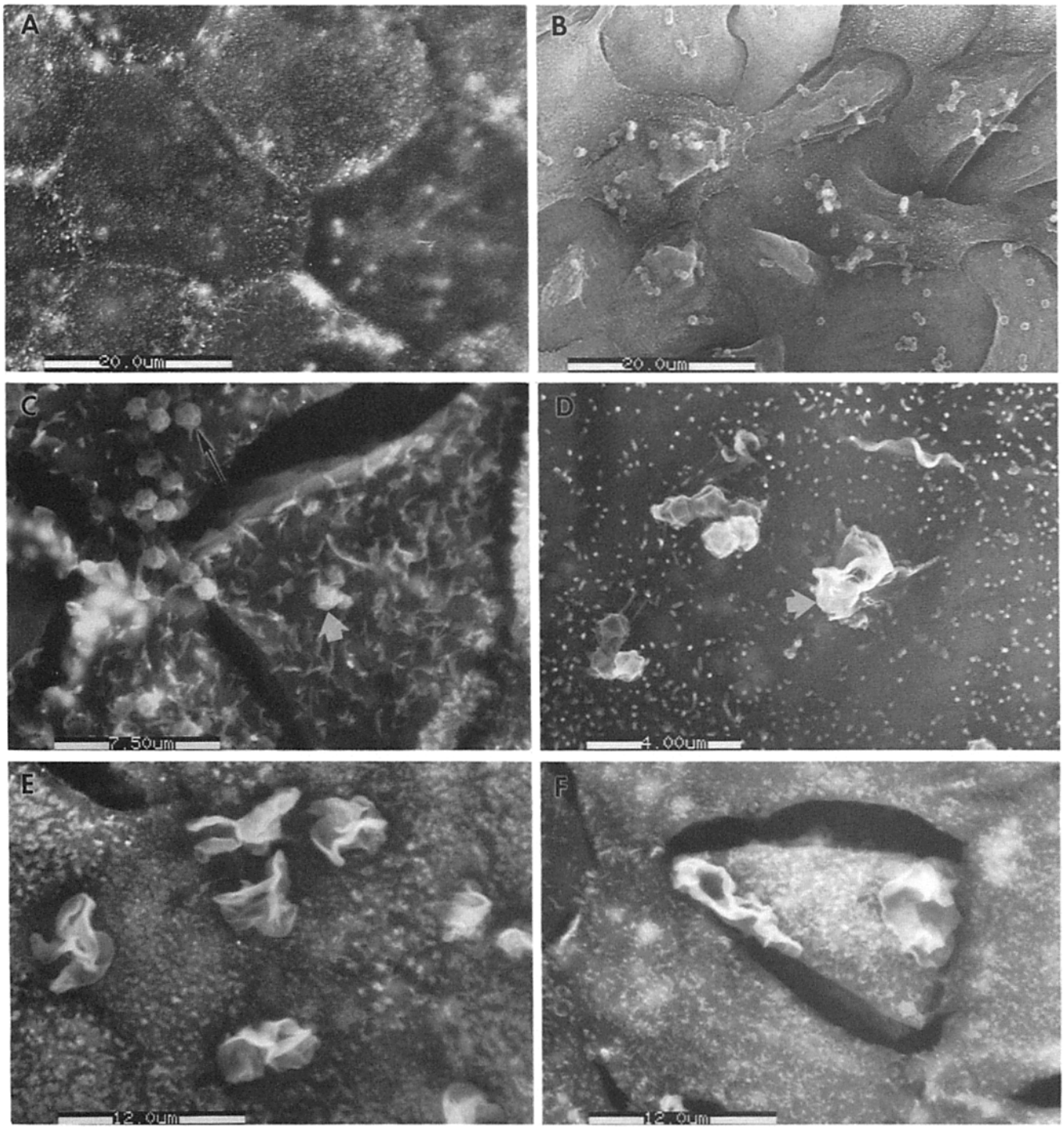

Figure 11. Scanning electron micrographs showing cell shape changes and surface features of cultured thyroid cells. (*A*) Control culture shows a monolayer of polygonal cells with variable densities of microvilli. (*B*) Cells treated with TPA for 30 min in the presence of 0.04% suspension of carboxylate-latex beads shows a dramatic change in shape. Beads adhere to the cell surface but phagocytotic structures are rarely present. (*C–F*) Cells treated with TSH for 30 min in the presence of beads. In *C*, beads adhere to the cell surface (*black arrow*), and small ruffles and pseudopodial structures are present. Beads are trapped by ruffles (*white arrowhead*), and an example of bead entrapment (*white arrowhead*) is shown at higher magnification in *D*. Examples of the surface ruffles and pseudopods extended upon TSH treatment are shown in *E* and *F*; note the dramatic cell retraction associated with the development of dorsal protrusions (*F*).

tral actomyosin complexes participate in the shape changes and motility of cells treated with TPA, which differ from phagocytic activities observed with TSH. However, TPA may induce the formation of a myosin network in the dorsal cell region which is somewhat similar to that in TSH-treated cells.

Unlike the classic Ca^{2+}/calmodulin-dependent phosphorylation of MLC in smooth muscle and many nonmuscle cells

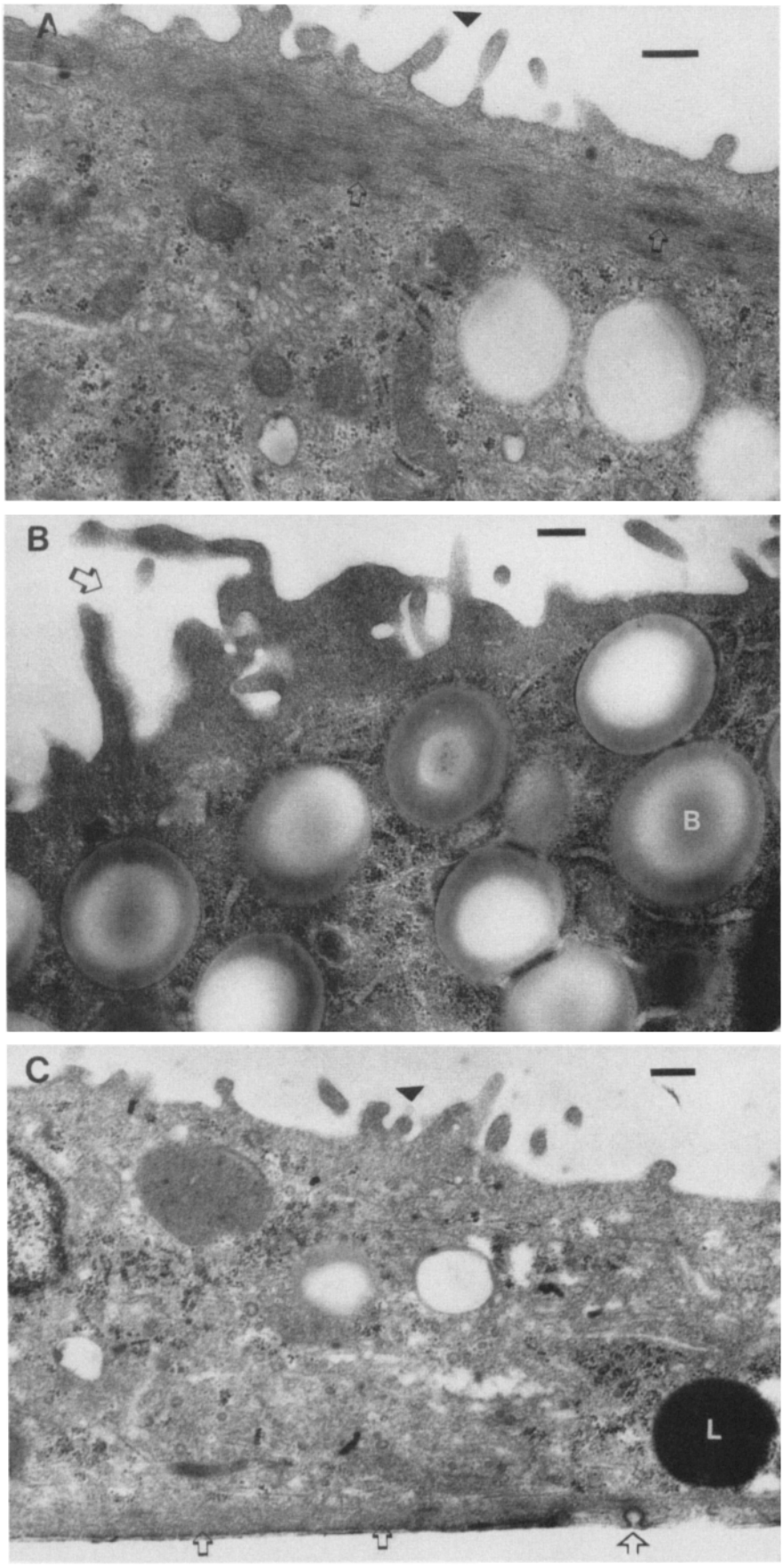

Figure 12. Electron micrographs of cultured thyroid cells exposed to carboxylate-latex beads. Confluent cell monolayers in 5H media were incubated with a 0.04% suspension of 1 μm carboxylate-latex beads for 30 min either without agents (control) (*A*), 40 mU/ml TSH (*B*), or 0.2 μM TPA (*C*), at 37°C, and prepared for transmission EM as described in Materials and Methods. In *A*, black arrowhead points to dorsal surface and protruding microvilli; beneath the plasma membrane, open arrows point to a parallel bundle of F-actin containing periodic, densely stained foci. *B* shows a region of a TSH-treated cell with a dorsal phagocytotic structure (*arrow*) and several ingested latex beads in the absence of stress fibers. In *C*, black arrowheads point to dorsal surface and microvilli of a TPA-treated cell. Arrows point to a parallel bundle of F-actin above the ventral membrane close to which is a coated pit (*open arrowhead*). *L*, lysosome; *B*, latex bead. Bars, 0.3 μm.

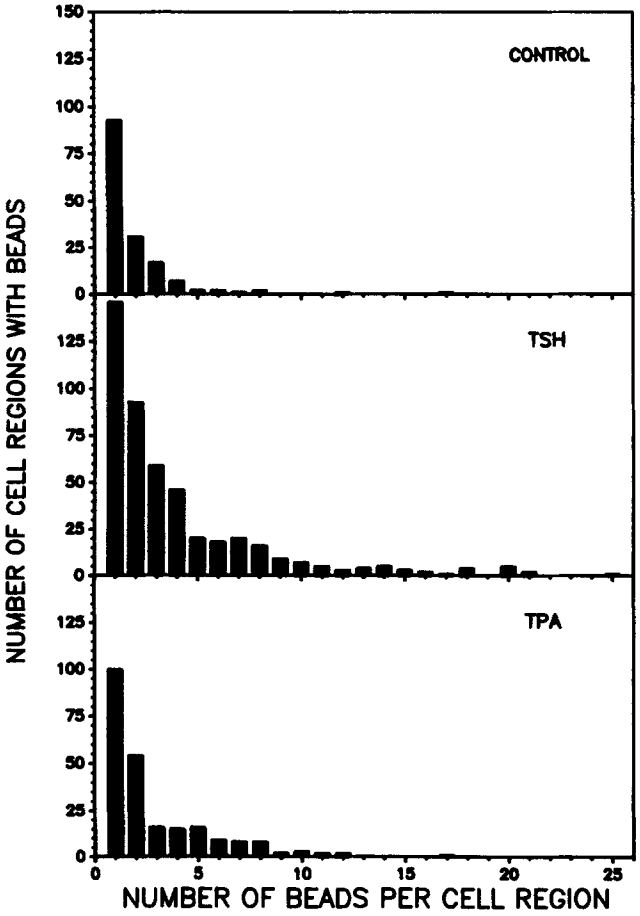

Figure 13. Quantitation of latex bead ingestion by cultured thyroid cells. Thick (1 μm) sections were cut vertically 70 μm apart from cell cultures (untreated controls, TSH or TPA treated) also prepared for transmission EM in Fig. 12. 2,500 cell regions, each being from a different cell, were examined for the three conditions, and intracellular beads were scored using phase contrast microscopy; a cell region is a vertical, 1-μm-thick section of a single cell. The total number of beads counted per condition was: 308 (*control*), 1,869 (*TSH*), and 681 (*TPA*).

(1, 4, 31, 56), phosphorylation of dog thyroid MLC does not appear to involve a Ca^{2+}-dependent kinase(s). In support of this, both EGTA and calmodulin inhibitors have little to no effect on ^{32}P-labeling of MLC in cell homogenates incubated with [γ-^{32}P]ATP. Similar phosphorylation activity is also found associated with the Triton-insoluble cytoskeletal fraction, suggesting a close spatial relationship between kinase and MLC. MLCK has been localized by immunofluorescence on the microfilament complex in 3T3 fibroblasts (20). Proteolytic conversion of Ca^{2+}-dependent kinase to a Ca^{2+}-independent form does not appear to be responsible for the phosphorylation characteristics in thyroid cells since protease inhibitors are present, and no such alteration is evident in the Ca^{2+}/calmodulin-dependent phosphorylation of a single 20-kD MLC species in thyroid fibroblast homogenates under the same buffer conditions. Interestingly, ^{32}P-MLC labeled in intact, basal thyroid cells contains a significant amount of phosphothreonine which has not typically been reported in other cell systems, although Ca^{2+}-independent threonine phosphorylation has been reported for brain MLC, which also is present in two species (36). Furthermore, in vitro phosphorylation of tyrosine has been observed in smooth muscle MLC (19), and phosphotyrosine is detected to a minor extent in thyroid. 2-D tryptic peptide mapping and phosphoamino acid analysis indicate that the major ^{32}P-peptide corresponds to the phosphopeptide containing the classic MLCK threonine 18 and serine 19 sites; there is no indication that serine 19 alone is phosphorylated to a significant extent in this study. Analyses of the two minor phosphopeptides indicate that they correspond to the peptides containing phosphoserine 1 or 2, and 1 and 2 (28). While TPA treatment of thyroid cells does not enhance C-kinase phosphorylation at these sites, the phosphorylation at such sites in addition to the MLCK sites, particularly after phosphatase inhibition by calyculin A, strongly suggests that various kinases (e.g., cyclin-p34^{cdc2}) can act on MLC in concert. Interestingly, a 20-kD MLC species is phosphorylated by a Ca^{2+}/calmodulin-dependent kinase in preparations from bovine thyroid tissue (51), and only a single species is observed in cultured bovine thyroid cells. It therefore appears that different molecular components and regulatory mechanisms exist, even among thyroid cytoskeletal systems.

One potential mechanism for the TSH-induced, cAMP-mediated decrease in the phosphorylation state of MLC is phosphorylation and subsequent inhibition of MLCK by A-kinase, which would result in net MLC dephosphorylation via phosphatase activity. This mechanism appears to operate in regulating the phosphorylation state of MLC in retinal cones when intracellular levels of cAMP are elevated (9). An even more definitive, direct demonstration of phosphorylation and inhibition of MLCK via A-kinase has been reported in fibroblasts (33). However, such a pathway does not appear to exist for the Ca^{2+}-independent MLCK in the dog thyroid system. MLC phosphorylation in cell homogenates or cytoskeletal preparations is not affected by the inclusion of cAMP with or without purified A-kinase, even though phosphorylation of several proteins was enhanced. Thus, this MLCK appears to lack both regulation by Ca^{2+}/calmodulin as well as an inhibitory A-kinase phosphorylation site.

Dephosphorylation of MLC induced by TSH (via cAMP) or the phorbol ester, TPA, appears to result from enhanced phosphatase activity, since MLC can be hyperphosphorylated upon addition of the phosphatase 1 and 2A inhibitor, calyculin A, after treatment of cells with these agents. Furthermore, calyculin A treatment alone increases MLC phosphorylation severalfold causing extensive actomyosin and cell contraction. Interestingly, phosphatase type-1 has been shown to localize on stress fibers and dephosphorylate MLC in fibroblasts (16). Phosphorylated MLC associated with the cytoskeletal fraction of Triton-lysed thyroid cells can be readily dephosphorylated (>90%) upon incubation in a Tris buffer system. This nearly complete and relatively specific dephosphorylation reflects that observed in intact cells treated with TSH, supporting the involvement of the same phosphatase(s). It is possible that stimulated phosphatase activity occurs by either direct phosphorylation of the phosphatase or inactivation of an inhibitor via A-kinase-mediated phosphorylation. For example, a protein phosphatase 1_M associated with myosin has been identified in rabbit skeletal muscle, and is inhibited by inhibitor-2; glycogen synthase kinase 3-mediated phosphorylation of inhibitor-2 inactivates

it, thereby promoting phosphatase activity (10). However, the rate and extent of thyroid MLC dephosphorylation was not affected by the addition of ATP, cAMP and purified A-kinase, suggesting that the regulatory element(s) is either not associated with the detergent-insoluble cytoskeletal fraction or is altered (data not shown). Inappropriate buffer conditions could also account for the lack of hypothetical cAMP-mediated stimulation of phosphatase activity in vitro.

In the present study, distinct differences relative to various other cell systems are observed in the state of cytoskeletal MLC phosphorylation and its regulation in response to cell agonists. MLC phosphorylation at serine 19 and threonine 18 by Ca^{2+}/calmodulin-dependent MLCK in smooth muscle or many nonmuscle cells correlates well with agonist-induced actomyosin contraction and subsequent functional events such as changes in cell shape or secretion. On the other hand, phagocytosis of latex beads induced by TSH and cAMP analogs, is associated with MLC dephosphorylation, apparently via A-kinase mediated stimulation of phosphatase activity. Although stimulation of C-kinase by TPA treatment might cause similar MLC dephosphorylation and actomyosin rearrangement in the dorsal cell region, it does not promote significant phagocytic activity. MLC dephosphorylation therefore appears to play at least a partial role in structural rearrangements of the actin/myosin-II cytoskeleton (16, 33); these altered complexes could provide a more flexible environment for cAMP-induced endocytotic structures and functions. Recently, long term exposure of cultured thyroid cells to γ interferon has been reported to reduce F-actin cytoskeletal complexes, part of which may be involved in microvilli and pseudopod structure since a dramatic decrease is observed in both microvilli number and TSH stimulation of pseudopod formation (6). Considering the consensus in the literature that MLC phosphorylation by MLCK is required for actomyosin contraction (3, 13, 31, 54), our observations of MLC dephosphorylation do not implicate an "active" role for myosin-II in pseudo-podial activities. It is possible, however, that localized actin polymerization, phosphorylation of myosin-I, and membrane interactions between F-actin and myosin-I (39) operate in thyroid phagocytosis.

The authors appreciate Ms. Donna Turner's work involving transmission EM procedures. We also are grateful to Drs. James B. Field and Masahiro Ikeda for their pioneering academic input related to this project.

This work was supported by the U.S. Public Health Service grant DK26088 from the National Institutes of Health and by grant DCB-8820262 from the National Science Foundation.

Received for publication 27 February 1992 and in revised form 25 March 1993.

References

1. Adelstein, R. S. 1982. Calmodulin and the regulation of the actin-myosin interaction in smooth muscle and nonmuscle cells. *Cell.* 30:349–350.
2. Adelstein, R. S., and M. A. Conti. 1975. Phosphorylation of platelet myosin increases actin-activated myosin ATPase activity. *Nature (Lond.).* 256:597–598.
3. Adelstein, R. S., M. D. Pato, and M. A. Conti. 1981. The role of phosphorylation in regulating contractile proteins. *Adv. Cyclic Nucleotide Res.* 14:361–373.
4. Aksoy, M. O., D. Williams, E. M. Sharkey, and D. J. Hartshorne. 1976. A relationship between Ca^{2+} sensitivity and phosphorylation of gizzard acto-myosin. *Biochem. Biophys. Res. Commun.* 69:35–41.
5. Anderson, N. L., and N. G. Anderson. 1977. High resolution two-dimensional electrophoresis of human plasma proteins. *Proc. Natl. Acad. Sci. USA.* 74:5421–5425.
6. Asakawa, H., J.-I. Miyagawa, T. Hanafusa, H. Katsura, A. Miyazaki, A. Otsuka, C. Nakagawa, K. Yamagata, K. Tajima, K. Mashita, N. Kono, and S. Tarui. 1990. Interferon-γ reduces actin filaments and inhibits thyroid-stimulating hormone-induced formation of microvilli and pseudopods in mouse monolayer thyrocytes. *Endocrinology.* 127:325–329.
7. Barany, K., S. Csabina, and M. Barany. 1985. The phosphorylation of the 20,000-Dalton myosin light chain in rat uterus. *In* Advances in Protein Phosphatase. W. Merlevede and J. DiSalvo, editors. Vol. II. 37–58.
8. Beeman, K., and T. Hunter. 1978. Characterization of rous sarcoma virus src gene products synthesized in vitro. *J. Virol.* 28:551–566.
9. Bernside, B., and N. Ackland. 1987. Calcium-independent contraction in lysed cell models of teleost retinal cones: Activation by unregulated myosin light chain kinase or high magnesium and loss of cAMP inhibition. *J. Cell Biol.* 105:397–402.
10. Chisholm, A. A. K., and P. Cohen. 1988. Identification of a third form of protein phosphatase 1 in rabbit skeletal muscle that is associated with myosin. *Biochim. Biophys. Acta.* 968:392–400.
11. Cole, H. A., H. S. Griffiths, V. B. Patchell, and S. V. Perry. 1985. Two-site phosphorylation of the phosphorylatable light chain (20-kDa light chain) of chicken gizzard myosin. *FEBS (Fed. Eur. Biochem. Soc.) Lett.* 180:165–169.
12. Conti, M. A., and R. S. Adelstein. 1981. The relationship between calmodulin binding and phosphorylation of smooth muscle myosin kinase by the catalytic subunit of 3':5' cAMP-dependent protein kinase. *J. Biol. Chem.* 256:3178–3181.
13. Cooke, R., and J. T. Stull. 1981. Myosin phosphorylation. *In* Cell and Muscle Motility. R. M. Dowben and J. W. Shay, editors. Plenum, New York. Vol. I. 99–133.
14. Dedman, J. R., B. R. Brinkley, and A. R. Means. 1979. Regulation of microfilaments and microtubules by calcium and cyclic AMP. Adv. Cyclic Nucleotide Res. 11:131–174.
15. Dunbar, B. S. 1986. Protein analysis using high-resolution two-dimensional polyacrylamide gel electrophoresis. *In* Laboratory Methods Manual for Hormone Action and Molecular Endocrinology, Tenth Edition. W. T. Schrader and B. W. O'Malley, editors. Houston Biological Assoc., Publishers, Houston, TX. 15:1–36.
16. Fernandez, A., D. L. Brautigan, M. Mumby, and N. J. C. Lamb. 1990. Protein phosphatase type-1, not type-2A, modulates actin microfilament integrity and myosin light chain phosphorylation in living nonmuscle cells. *J. Cell Biol.* 111:103–112.
17. Fox, J. E. B., and D. R. Phillips. 1982. Role of phosphorylation in mediating the association of myosin with the cytoskeletal structures of human platelets. *J. Biol. Chem.* 257:4120–4126.
18. Gabrion, J., F. Travers, Y. Benyamin, P. Sentein, and N. V. Thoai. 1980. Characterization of actin microfilaments at the apical pole of thyroid cells. *Cell Biol. Int. Rep.* 4:59–68.
19. Gallis, B., A. M. Edelman, J. E. Casnellie, and E. G. Krebs. 1983. Epidermal growth factor stimulates tyrosine phosphorylation of the myosin regulatory light chain from smooth muscle. *J. Biol. Chem.* 258: 13089–13093.
20. Guerriero, V., D. R. Rowley, and A. R. Means. 1981. Production and characterization of an antibody to myosin light chain kinase and intracellular localization of the enzyme. *Cell.* 27:449–458.
21. Harrington, W. F., and M. E. Rodgers. 1984. Myosin. *Annu. Rev. Biochem.* 53:35–73.
22. Herring, B. P., and P. J. England. 1986. The turnover of phosphate bound to myosin light chain-2 in perfused rat heart. *Biochem. J.* 240:205–214.
23. Ikebe, M., D. J. Hartshorne, and M. Elzinga. 1985. Identification, phosphorylation, and dephosphorylation of a second site for myosin light chain kinase on the 20,000 Dalton light chain of smooth muscle myosin. *J. Biol. Chem.* 261:36–39.
24. Ikebe, M., M. Inagaki, K. Kanamaru, and H. Hidaka. 1985. Phosphorylation of smooth muscle myosin light chain kinase by Ca^{2+}-activated, phospholipid-dependent protein kinase. *J. Biol. Chem.* 260:4547–4550.
25. Ikebe, M., D. J. Hartshorne, and M. Elzinga. 1987. Phosphorylation of the 20,000-dalton light chain of smooth muscle myosin by the calcium-activated, phospholipid-dependent protein kinase. *J. Biol. Chem.* 262: 9569–9573.
26. Ikeda, M., W. J. Deery, T. B. Nielsen, M. S. Ferdows, and J. B. Field. 1986. Dephosphorylation of 19K and 21K polypeptides in response to thyroid-stimulating hormone in cultured thyroid cells. *Endocrinology.* 119: 591–599.
27. Ikeda, M., W. J. Deery, M. S. Ferdows, T. B. Nielsen, and J. B. Field. 1987. Role of cellular Ca^{++} in phosphorylation of 21K and 19K polypeptides in cultured thyroid cells: effects of phorbol ester, trifluoperazine, and 8-diethylamino-octyl-3,4,5-trimethoxybenzoate hydrochloride. *Endocrinology.* 121:175–181.
28. Kawamoto, S., A. R. Bengur, J. R. Sellers, and R. S. Adelstein. 1989. In situ phosphorylation of human platelet myosin heavy and light chains by protein kinase C. *J. Biol. Chem.* 264:2258–2265.
29. Kellie, S., T. C. Holme, and M. J. Bissell. 1985. Interaction of tumour promoters with epithelial cells in culture. *Exp. Cell Res.* 160:259–274.
30. Korn, E. D., and J. A. Hammer, III. 1988. Myosins of nonmuscle cells. *Annu. Rev. Biophys. Chem.* 17:23–45.

31. Kuznicki, J., and B. Barylko. 1988. Phosphorylation of myosin in smooth muscle and non-muscle cells. In vitro and in vivo effects. *Int. J. Biochem.* 20:559–568.
32. Laemmli, U. K. 1970. Cleavage of structural proteins during the assembly of the head of bacteriophage T4. *Nature (Lond.).* 227:680–685.
33. Lamb, J. C., A. Fernandez, M. A. Conti, R. Adelstein, D. B. Glass, W. J. Welch, and J. R. Feramisco. 1988. Regulation of actin microfilament integrity in living nonmuscle cells by the cAMP-dependent protein kinase and the myosin light chain kinase. *J. Cell Biol.* 106:1955–1971.
34. Langanger, G., M. Moeremans, G. Daneels, A. Sobieszek, M. De Brabander, and J. DeMey. 1986. The molecular organization of myosin in stress fibers of cultured cells. *J. Cell Biol.* 102:200–209.
35. Martin, F., J. Gabrion, and J. C. Cavadore. 1981. Thyroid myosin filament assembly-disassembly is controlled by myosin light chain phosphorylation-dephosphorylation. *FEBS (Fed. Eur. Biochem. Soc.) Lett.* 131: 235–238.
36. Matsumura, S., N. Murakami, S. Yasuda, and A. Kumon. 1982. Site-specific phosphorylation of brain myosin light chains by calcium-dependent and calcium-independent myosin kinases. *Biochem. Biophys. Res. Commun.* 109:683–688.
37. Nielson, T. B., M. S. Ferdows, B. R. Brinkley, and J. B. Field. 1985. Morphological and biochemical responses of cultured thyroid cells to thyrotropin. *Endocrinology.* 116:788–797.
38. Pearson, R. B., R. Jakes, M. John, J. Kendrick-Jones, and B. E. Kemp. 1984. Phosphorylation site sequence of smooth muscle myosin light chain (M_r = 20,000). *FEBS (Fed. Eur. Biochem. Soc.) Lett.* 168:108–112.
39. Pollard, T. D., S. K. Doberstein, and H. G. Zot. 1991. Myosin-I. *Annu. Rev. Physiol.* 53:653–681.
40. Rimm, D. L., D. A. Kaiser, D. Bhandari, P. Maupin, D. P. Kiehart, and T. D. Pollard. 1990. Identification of functional regions on the tail of Acanthamoeba myosin-II using recombinant fusion proteins. I. High resolution epitope mapping and characterization of monoclonal antibody binding sites. *J. Cell Biol.* 111:2405–2416.
41. Roger, P. P., F. Rickaert, F. Lamy, M. Authelet, and J. E. Dumont. 1989. Actin stress fiber disruption and tropomyosin isoform switching in normal thyroid epithelial cells stimulated by thyrotropin and phorbol esters. *Exp. Cell Res.* 182:1–13.
42. Sagara, J., K. Nagata, and Y. Ichikawa. 1982. A cofactor protein required for actin activation of myosin Mg^{2+} ATPase activity in leukemic myeloblasts. *J. Biochem.* 92:1845–1851.
43. Scheid, C. R., T. W. Honeyman, and F. S. Fay. 1979. Mechanism of B-adrenergic relaxation of smooth muscle. *Nature (Lond.).* 277:32–36.
44. Schliwa, M., T. Nakamura, K. R. Porter, and U. Euteneuer. 1984. A tumor promoter induces rapid and coordinated reorganization of actin and vinculin in cultured cells. *J. Cell Biol.* 99:1045–1059.
45. Scholey, M. J., K. A. Taylor, and J. Kendrick-Jones. 1980. Regulation of non-muscle myosin assembly by calmodulin-dependent light chain kinase. *Nature (Lond.).* 287:233–235.
46. Sellers, J. R., B. P. Chock, and R. S. Adelstein. 1983. The apparently negatively cooperative phosphorylation of smooth muscle myosin at low ionic strength is related to its filamentous state. *J. Biol. Chem.* 258: 14181–14188.
47. Sellers, J. R., J. A. Spudich, and M. P. Sheetz. 1985. Light chain phosphorylation regulates the movement of smooth muscle myosin on actin filaments. *J. Cell Biol.* 101:1897–1902.
48. Silberstein, L., and S. J. Lowey. 1981. Isolation and distribution of myosin isoenzymes in chicken pectoralis muscle. *J. Mol. Biol.* 148:153–189.
49. Suzuki, H., J. Onishi, K. Takanishi, and S. Watanabe. 1978. Structure and function of chicken gizzard myosin. *J. Biochem.* 84:1529–1542.
50. Takazawa, K., T. Endo, and T. Onaya. 1988. Phagocytotic activities of latex beads by FRTL cell: possible interaction of cell surface glycoprotein. *Acta Endocrinol.* 117:198–204.
51. Tawata, M., R. Kobayashi, and J. B. Field. 1983. Partial purification and characterization of myosin light chain kinase from bovine thyroid gland. *Endocrinology.* 112:701–706.
52. Tramontano, D., A. Avivi, F. S. Ambesi-Impiombato, L. Barak, B. Geiger, and J. Schlessinger. 1982. Thyrotropin induces changes in the morphology and the organization of microfilament structures in cultured cells. *Exp. Cell Res.* 137:269–275.
53. Trotter, J. A., S. P. Scordilis, and S. S. Margossian. 1983. Macrophages contain at least two myosins. *FEBS (Fed. Eur. Biochem. Soc.) Lett.* 156: 135–140.
54. Walsh, M. P., and D. J. Hartshorne. 1982. Actomyosin of smooth muscle. *In* Calcium and Cell Function. W. Y. Cheung, editor. Academic Press, New York. Vol. III. 223–269.
55. Westermark, B., and K. R. Porter. 1982. Hormonally induced changes in the cytoskeleton of human thyroid cells in culture. *J. Cell Biol.* 94:42–50.
56. Yerna, M. J., R. Dabrowska, D. J. Hartshorne, and R. D. Goldman. 1979. Calcium-sensitive regulation of actin-myosin interactions in baby hamster kidney (BHK-21) cells. *Proc. Natl. Acad. Sci. USA.* 76:184–188.